[AMERICAN JOURNAL OF SCIENCE, VOL. 298, APRIL, 1998, P. 324–347]

PRESERVATION OF $\delta^{18}O$ AND $\delta^{13}C$ IN BELEMNITE ROSTRA FROM THE JURASSIC/EARLY CRETACEOUS SUCCESSIONS

OLAF G. PODLAHA*, JÖRG MUTTERLOSE, and JÁN VEIZER**
Institut für Geologie, Ruhr-Universität Bochum, 44780 Bochum, Germany

ABSTRACT. Stratigraphic collection of 263 belemnite rostra (guards) from Jurassic to Lower Cretaceous sediments in the Moscow area of Russia, northern Germany, England, New Zealand, and Morocco were analyzed to determine temporal variations in their $\delta^{18}O$ and $\delta^{13}C$ as a proxy for isotopic composition of surface seawater. Internal structures of the rostra were studied using cathodoluminescence and SEM techniques, their trace element (Fe, Mn, Mg, and Sr), and the stable carbon and oxygen isotope compositions. The average stratigraphic resolution is about 1 Ma. These samples represent a broad range of paleolatitudes and paleoceanographic settings, ranging from 42°N to 82°S, covering boreal to subtropical, brackish to open marine shelf paleoenvironments.

The rostra originally contained domains enriched in organic matter that were later replaced by luminescent diagenetic calcite, thereby generating an impression of "seasonal growth rings." Diagenetic calcite accounts for up to 6.8 percent of the rostrum. The trace element content of the rostra range from 227 to 3935 ppm for Mg, 379 to 1514 ppm for Sr, and up to 305 and 3662 ppm for Mn and Fe, respectively. However, selective drilling of only primary calcitic domains resulted in 90 percent of all analyzed samples to fall within the range of trace element values typical for modern low Mg-calcite shells. The chemical and textural data suggest that the primary calcite of the rostra is well preserved, as is its isotopic signature.

The $\delta^{13}C$ and $\delta^{18}O$ measurements define oscillating temporal bands, of about 3 to 4 permil width, around more or less modern marine values of +2 and −1 permil, respectively. Oxygen isotopes in the well preserved rostra most likely reflect temperature variations within a $\sim 14 \pm 8$°C range. The observed 3 to 4 permil spread of values between contemporaneous specimens, which is comparable to the scatter of data reported for modern low-Mg calcitic brachiopod shells, probably reflects the diversity of local ecosystems, although some of the spread may be due to real short term temporal variations within single biozones. The $\delta^{13}C$ values of the rostra define a band similar to that of the oxygen isotopes, and the temporal oscillations of both isotope curves are commonly in phase.

The above dataset, complemented by the results of Jones, Jenkyns, and Hesselbo (1994) and Jones and others (1994), yields a composite $\delta^{18}O$ and $\delta^{13}C$ variations in belemnite guards for the entire Jurassic-Early Cretaceous interval. For $\delta^{18}O$, the oscillating band indicates that the most negative values occur at times of independently postulated global and/or regional anoxic events, such as those in the Toarcian and Kimmeridgian as well as the Aptian. These OAEs appear to be characterized by up to 10°C higher seawater temperatures than the intervening background times. The $\delta^{13}C$ record shows ^{13}C depletion for the Kimmeridgian event but enrichment for the other two, suggesting that the $\delta^{13}C$ temporal oscillations and OAEs are not simply a reflection of surficial productivity due to operation of the biological pump, but rather of changing oceanic circulation patterns due to variations in latitudinal surface temperature gradients.

* Present address: Shell International Exploration and Production, Research and Technical Services, Volmerlaan 8, 2280 AB Rijswijk, The Netherlands
** Also: Ottawa-Carleton Geoscience Center, Department of Geology, University of Ottawa, Ottawa, Ontario K1N 6N5, Canada

INTRODUCTION

Since the original studies of Bøggild (1930) the succession of concentric rings in calcitic belemnite rostra has been believed to represent primary growth texture formed by alteration of laminae pellucidae and laminae obscurae (Müller-Stoll, 1936). Accepting this interpretation, Urey and others (1951) explained the variations in $\delta^{18}O$ between bands as seasonal temperature gradients, thereby establishing the stable isotope geochemistry as a potential tool for paleoclimatic studies. Considering these oscillating isotopic patterns, Longinelli (1969) and Spaeth, Hoefs, and Vetter (1971) proposed that belemnites had a life span of some 5 to 10 yrs. Further studies by Veizer (1974) and Veizer and Fritz (1976) showed, however, that such "seasonal" isotope variations appeared to have been more pronounced in samples that contained some indications of recrystallization and that oxygen isotope paleotemperature estimates (Fritz, 1967) were at odds with paleoclimatic interpretations based on lithological and faunal criteria. These authors also demonstrated that the oxygen isotope signal suffered post-depositional resetting, principally due to precipitation of up to 10 percent diagenetic calcite into rostra pore spaces. Similarly, Spaeth (1975) proposed, from analogy with skeletal texture of its closest living relative sepia, that belemnite rostra may have had up to 20 percent primary porosity.

An alternative model for the structure of belemnite rostra was proposed by Sælen (1989). In his view, the laminae obscurae were originally porous and contained organic matter. Postmortally, this organic matter decayed and was replaced by diagenetic calcite, thus generating a pattern resembling primary "growth rings."

The issue of oxygen isotopic composition of the Mesozoic and older seawater is one of the hotly debated subjects of isotope geology. One school flatly disputes that an original marine isotope signal in such old calcites can ever be preserved (Land, 1995 versus Veizer, 1995). Others, while accepting the possibility of signal preservation, disagree as to the causes of the observed ^{18}O depletion in the course of the Phanerozoic. Their explanations range from changing isotopic composition of past seawater to progressively warmer and/or more stratified ancient oceans (for reviews, see Popp, Anderson, and Sandberg, 1986; Veizer, Fritz, and Jones, 1986; Hudson and Anderson 1989; Corfield, 1995; Veizer and others, 1997).

In contrast to the Paleozoic, the stable isotope record for Mesozoic carbonates (Degens and Epstein, 1962; Weber, 1967; Veizer and Hoefs, 1976) suggests that their $\delta^{18}O$ and $\delta^{13}C$ compositions were not markedly different from their Quaternary counterparts, either in terms of averages or in the spread of values, the latter reflecting the diversity of natural environmental variables. This large spread of isotopic values was observed also in the pioneering studies of Jurassic and Early Cretaceous belemnites (Bowen, 1966; Fritz, 1967; Brennecke, 1977) and attributed to their broad regional and stratigraphic framework. The recent studies of Jones, Jenkyns, and Hesselbo (1994) and Jones and others (1994) aimed specifically at the development of a detailed Sr isotope curve and have thus the required high resolution. Yet, even these show a dispersion of stable isotope values of several permil for any given time period. The question arises whether this is an inherent feature of the low-Mg calcitic belemnite rostra, as in the modern brachiopods (Carpenter and Lohmann, 1995). If so, does it reflect paleoenvironmental parameters (compare Lowenstam, 1961) or the hypothesized species specific isotopic fractionation (Sælen and Karstang, 1989)? In other words, can belemnite guards be utilized as proxies for high resolution paleoceanographic studies?

Quantification of these phenomena is a prerequisite if we are to extend the success of the Quaternary and Tertiary isotope studies based on foraminifera (Emiliani and Shackleton, 1974; Shackleton and Kennett, 1975; Woodruff, Savin, and Douglas, 1981; Ruddiman and others, 1989) to the Mesozoic. In this contribution, we aim to document

that application of suitable experimental techniques can potentially yield results comparable to those based on Cenozoic foraminifera.

GEOLOGICAL SETTING OF SAMPLES

For this project, 263 belemnite rostra were studied by cathodoluminescence (and in part by SEM) in order to decipher their internal texture. They were further analyzed for trace elements and for isotopes of oxygen, carbon, and strontium (Podlaha, 1995). Here we shall discuss all these parameters, with the exception of Sr isotopes.

The belemnite rostra were collected from several institutional and private collections as well as in the field. The locations and taxonomic assignment of samples are listed in app. 1. The sampling strategy was to try to cover all biozones of the Middle Jurassic through Early Cretaceous time interval. For the sake of simplicity, the discussion in the subsequent text will be based only on stratigraphic stages, but the specific biozone for each sample can be found in app. 1.

The studied field sections and their lithologies are summarized in figure 1. In terms of paleogeography, the sections cover a large paleolatitudinal range (Smith, Hurley, and Briden, 1981) from 42°N (Russia), to 42° to 38°N (England and northern Germany), 28°N (Morocco), and 82°S (New Zealand). The Russian platform localities were a part of shallow marine coastal sedimentary environment with boreal affinities. During the Late Jurassic and Early Cretaceous this environment was characterized by several transgressions from Tethyan as well as boreal realms (Dolginow and Kropatschjew, 1994). The Jurassic sections sampled in northern Germany were originally deposited under boreal climates in a shallow marine embayment of the proto-North Sea basin. The Berriasian localities of northern Germany and England were dominated by terrigeneous brackish sedimentation of the "Wealden" facies. From Valanginian to Aptian time, the study areas in southern England were partially closed basins with brackish sedimentation, while boreal marine conditions prevailed in northeastern England and northern Germany (Mutterlose, 1992). The Barremian samples from Morocco came with only biostratigraphic information, however, most of the latest Early Cretaceous sediments in these regions are dominated by successive shallow marine marl-limestone sequences (Wiedmann, Butt, and Einsele, 1978; Thurow and Kuhnt, 1986). On the other hand, Late Jurassic sections from New Zealand were deposited in marginal basins that, in addition to marine influence from the Pacific, also contain intercalations of terrestrial facies sourced from Australia (Fleming and Kear, 1960; Helby, Wilson, and Grant-Mackie, 1988).

PREPARATION TECHNIQUES

The early geochemical studies of belemnite rostra (Longinelli, 1969; Milliman, 1974; Spaeth, Hoefs, and Vetter, 1971; Jones, Jenkyns, and Hesselbo, 1994; Jones and others, 1994) utilized pre-treatment by hydrochloric or acetic acid to dissolve secondary phases, such as diagenetic calcites. In this work, we employed a different preparation technique. First, the rostra were cleaned in an ultrasonic bath. Each rostrum was then cut dorsoventrally perpendicular to its length (fig. 2). A double polished thin section was prepared for cathodoluminescence (CL), and half the remaining rostra cut again perpendicular to its length. The resulting middle slice was stored for later analytical work. One portion of the apex segment was treated for 3 min in 1 percent HCl, the etched surface utilized for SEM studies (fig. 2).

For CL work, we have utilized a self-constructed, petrological CL-microscope with a hot cathode (Neuser, 1988). With this apparatus, Mn concentrations as low as 15 to 20 ppm have been observed to excite CL (Richter and Zinkernagel, 1980), providing that Fe concentrations were low (compare Savard, Veizer, and Hinton, 1995; Bruhn and

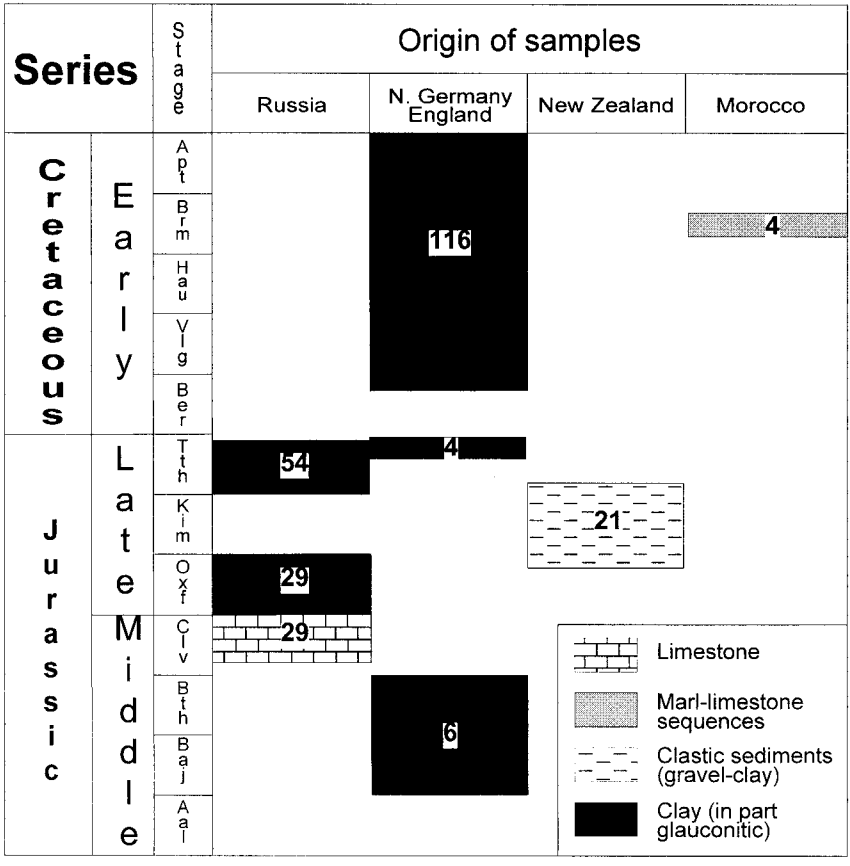

Fig. 1. Lithology and stratigraphic range of the sections sampled (4-116 are the number of samples). Jurassic profiles from Germany (samples provided by C. Spaeth) do not have locations specified. The late Jurassic profile from Russia (sampled in the field) include Russia I = Voskresjensk N9-2bis, Russia II = Voskresjensk N7-2bis, Russia III = Ribinsk, and Russia IV = Jaroslawskaja. The Late Jurassic profiles from New Zealand (samples provided by A. B. Challinor and R. S. Stevens) are from Kawhaia Harbor. The Early Cretaceous profiles from Northern Germany (samples provided by J. Mutterlose) include the localities Diepenau, Engelbostel, Frielingen, Gott, and Moorberg. The Early Cretaceous profile from England (samples provided by J. Mutterlose) is from Speeton. The Early Cretaceous profile from Morocco (samples provided by J. Mutterlose) is from Agadir.

others, 1995). The SEM observations were made on a Cambridge Instrument, with an acceleration voltage of 20 kV.

The middle segment of the rostrum was initially back-illuminated and drilled with 0.25 or 0.5 mm bits. In a later research phase, we have utilized a dental core drill with an external diameter of 0.3 mm. Drill bits were washed between samples in acetone, ethanol, and in an ultrasonic bath. Ideally, we attempted to drill within a single lamina pellucida. For test purposes, we also sampled the secondary diagenetic calcite of the apical line region. We opted for this approach, because the previously utilized acid pre-treatment technique preferentially attacked secondary phases, permitting infiltration of the contaminated acid into the interior of the rostra along microfractures. Since each rostrum is characterized by its own peculiarities, it is difficult to guarantee the reproducibility of this procedure between samples.

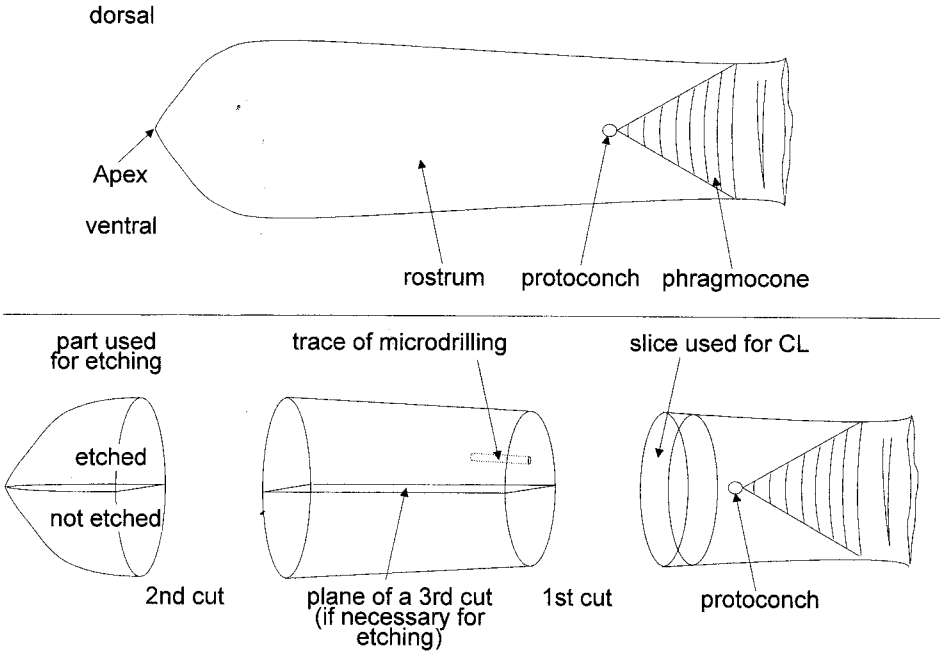

Fig. 2. Schematic representation of sample preparation for optical and geochemical studies.

The powder aliquot obtained by drilling or by pulverizing the drillcore in an agate mortar was then utilized for determination of oxygen and carbon isotopic compositions. The samples were analyzed on Finnigan MAT 251 and Finnigan MAT DELTA S mass spectrometers at the Institute for Geology, Ruhr-University, Bochum. The external reproducibility, based on duplicates, was 0.18 and 0.24 permil for the $\delta^{13}C$ and $\delta^{18}O$, respectively (for further details see Bruckschen and Veizer, 1997). Ca, Mg, Sr, Mn, and Fe concentrations were determined on a Philips PU 7000 ICP-AES spectrometer, using the diluted phosphoric acid that remained after dissolution of carbonates for stable isotope preparation (compare Coleman, Walsh, and Benmore, 1989). Since the phosphoric acid cannot be regained fully (~75 percent) from the Y-tube reaction vessel to the ICP, the trace element concentrations were normalized by a factor needed to adjust the ICP calcium values to 40 wt percent. Two blind samples were measured with each set of 18 samples. The advantage of this approach is that the trace element data originate from the same aliquot as the isotope results. The ICP measurements, particularly for Sr and Mn, showed a good agreement with the PIXE data (Bruhn and others, 1995). The mean accuracy of the measured chemical data is better than 99.1 percent compared to standard, and the mean reproducibility for individually prepared material of the same rostrum is 99 percent. All experimental results are listed in app. 2.

MICROTEXTURE OF THE ROSTRA

The primary microtexture of the guard is that of radially-arranged calcite prisms. The guards often show variable stages of recrystallization with large, radially oriented crystals attaining sizes up to the radius of the guard (fig. 3). Irregular tooth-like intercalations and impurities at grain boundaries suggest that this is a result of grain coarsening. The coarsening process may be driven by diminished solubility due to

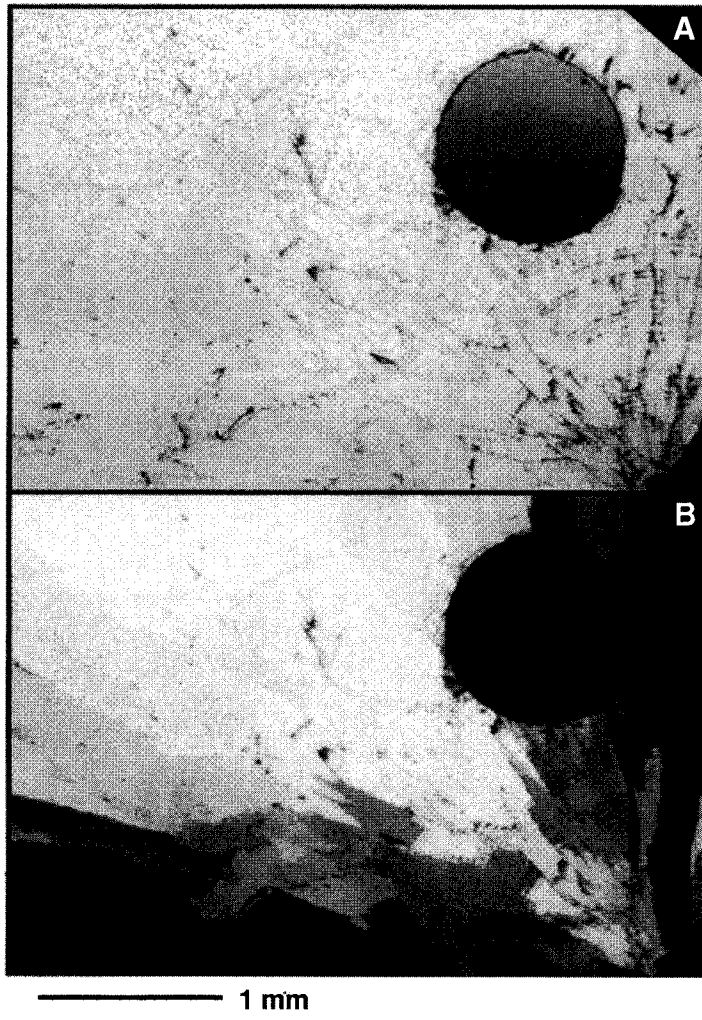

Fig. 3. View of the rostra under transmitted light. The circular drilling hole has a diameter of 1 mm. (A) Polarized light. The "contaminated" recrystallized grain boundaries are clearly visible. (B) Crossed nicols. The radial crystal orientation is visible despite recrystallization.

energetic reasons, or the texture may be a result of relaxation or of a thermal retrograde process. We believe (Podlaha, 1995) that the first alternative is the most likely possibility.

INTERNAL STRUCTURE UNDER CL AND SEM

The essential feature of the internal structure of belemnite rostra under CL and SEM were previously described by Sælen (1989). We shall therefore discuss only the observations specific to this study.

Many calcites, particularly those of secondary origin, are characterized by yellow-orange-red luminescence that is activated by Mn^{2+} (Richter and Zinkernagel, 1980; Machel, 1985; Reeder and Grams, 1987; Savard, Veizer, and Hinton, 1995). Ninety percent of the rostra studied have shown only a bluish intrinsic luminescence, with the

remaining 10 percent having a weak yellow luminescence. The generally low Mn^{2+} (and Fe^{2+}) concentrations measured in the rostra (app. 2) are in accord with this observation. In the black and white photographs (fig. 4) intrinsic fluorescence is seen as a dark-gray shade.

Samples that were etched with HCl for SEM studies show that the purer portions of the rostra were leached preferentially. In contrast, those portions of the rostra that contain higher Fe and/or Mn concentrations (Sælen, 1989) and are luminescent under CL (fig. 5) stand out as topographic ridges or "growth" rings. The domains that show dark-violet luminescence, due to dispersed intracrystalline organic material, appear as radial calcite prisms with coarser surface under SEM.

Characterizing the rostra by CL and SEM, we estimate that secondary calcite accounts, on average, for about 2 ± 1.3 percent (2σ) of the observed cross sections, but it can vary from 0 to 6.8 percent. This is close to 10 percent maximum porosity of rostra suggested by Veizer (1974) based on trace element partitioning, but it is considerably less than the value of 20 percent suggested by Spaeth (1975) by analogy with the sepia skeleton. The pattern of concentric "growth" rings that is formed by the secondary calcite varies from one specimen to another (Sælen, 1989; Spaeth, Hoefs, and Vetter, 1971) and is not species specific (figs. 4, 5). This secondary calcite may represent an infill

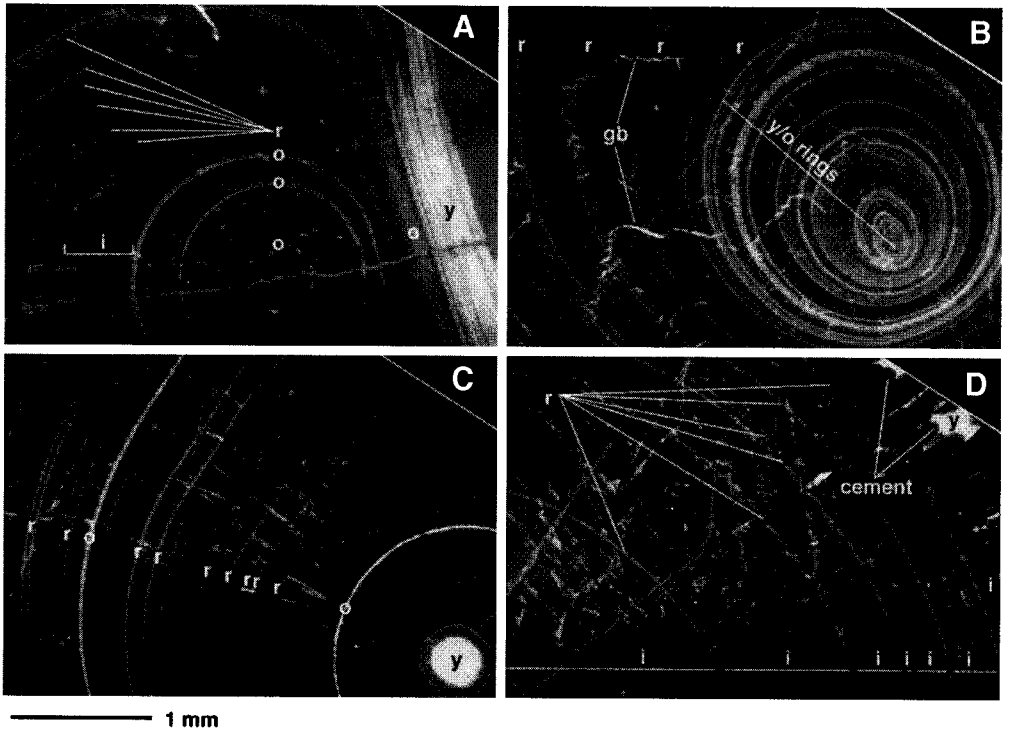

Fig. 4. Examples of belemnite rostra with variable CL characteristics. All examples are from the 10 percent of samples that showed CL. A. Cross section with 3 types of luminescence: red (r), orange (o), and yellow (y). The section with the intrinsic luminescence is marked (i). A fanning sequence of compact luminescent layers is visible between the apical line and the ventral furrow (see also fig. 5C). B. Cross section showing, in addition to the previously described features (A), also clearly recrystallized grain boundaries (gb). C. Cross section with luminescent rings and with diagenetic cements in the apical line domain. D. Cross section with diagenetic cement in corrosion pits. The rostrum itself shows only a subdued luminescence.

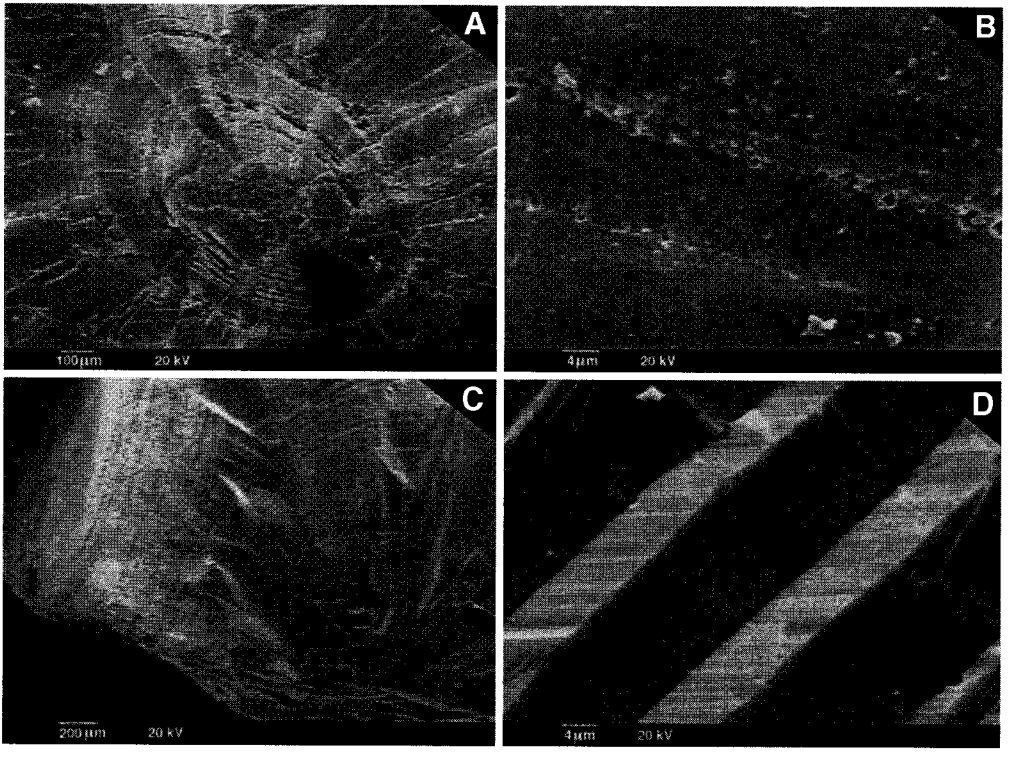

Fig. 5. SEM pictures of corrosion pits. (A) domain around the apical line; (B) rings of secondary calcites; (C) etched cross section with rings of secondary calcite (see also fig. 4A); (D) massive calcite prisms with compact lamination.

of an original porosity or of a secondary porosity created by the decaying organic matter, both concentrated in the "laminae obscurae." The observation that calcite in the volumetrically predominant "laminae pellucidae" shows no such porosity argues for the decay of organic matter as the likely reason for localization of secondary calcite in the rostra. This hypothesis is supported by the light $\delta^{13}C$ isotope ratios measured for domains enriched in secondary calcite (Podlaha, 1995).

CHEMICAL COMPOSITION OF THE ROSTRA

A comparison of the trace element data measured in the rostra (app. 2) with the concentrations encountered in modern marine LMC shells shows that the bulk of the samples cluster in the vicinity of the modern counterparts. Note, for example, that only 19 samples from the set of 263 show excess Mn values. Such clustering of chemical data suggests that the bulk of the belemnite rostra retained their near original chemical makeup, an observation in accord with the optical constraints. As a caveat, it should be kept in mind that the comparison with modern LMC marine shells are only approximations, since no living representatives of belemnites are available for comparison.

Some samples, however, do display features typical of post-depositional repartitioning, such as Sr and Mg depletions and Mn and Fe enrichments (compare Veizer, 1983; Brand, 1989; Banner, 1995). Statistical treatment of the data (table 1) confirms that Fe covaries with Mn, and Sr covaries with Mg, but the expected negative correlation

TABLE 1

Principal component analysis of chemical and isotope data for belemnite rostra (N + 263, rotated factor pattern)

	Factor 1	Factor 2	Factor 3	Factor 4
Mg/Ca		0.87		
Sr/Ca		0.84		
Mn/Ca	−0.89			
Fe/Ca	−0.83			
$\delta^{13}C$				0.58
$\delta^{18}O$				0.95
$^{87}Sr/^{87}Sr$			0.96	
% of Variance explained	24.8	21.2	16.5	18.8

between Mn and Sr (Brand and Veizer, 1980) is not evident in this dataset (fig. 6A). The absence of such negative relationship, combined with excellent textural preservation of the rostra, is consistent with the preservation of near to original trace element patterns.

ISOTOPE COMPOSITION OF THE ROSTRA

A picture similar to that of trace elements is presented also by the oxygen and carbon isotope data of the rostra. The bulk of the measurements cluster around the values comparable to those of present day marine calcite (fig. 7). Interestingly, the well and less well preserved samples, based on trace element criteria, show a comparable isotope scatter. These suggest, as did the CL and SEM studies, that even the majority of the samples identified as "altered" by trace element criteria are still quite well preserved in terms of their optical, chemical, and isotopic characteristics. Nonetheless, most of the rostra do show internal variability of up to 2 permil for both, $\delta^{18}O$ and $\delta^{13}C$ (fig. 8), particularly if the proportion of secondary calcite in the samples is high, such as in the region of the apical line or in domains with dense populations of "laminae obscurae." In contrast, the variability is much less in the well preserved specimens with dense grouping of "laminae pellucidae." The latter were exclusively drilled for this study. Optical, chemical, and isotope criteria demonstrate that the "cyclical seasonal" variations in $\delta^{18}O$ of the belemnite rostra (Urey and others, 1951; Longinelli, 1969; Spaeth, Hoefs, and Vetter, 1971) correlate with the presence of the luminescent secondary calcite. The observation of Longinelli (1969) that "seasonal" variations were more pronounced in recrystallized than in well-preserved specimens is thus not surprising. Furthermore, as discussed above, the domains of luminescent calcite are specific for individual rostra, they are not species dependent, and they do not represent regular growth rings. Such diagenetic domains are, in fact, entirely absent in the well preserved rostra that account for nine-tenths of our sample collection. It follows, therefore, that the proposed life span of 5 to 8 yrs for the belemnites (Spaeth, Hoefs, and Vetter, 1971), based on the "seasonal" variations in oxygen isotopes, may require reinterpretation as well.

Sælen and Karstang (1989) proposed that the $\delta^{18}O$ and $\delta^{13}C$ in belemnite rostra indicate species specific isotopic fractionation. Our results and data from Sælen, Doyle, and Talbot (1996) do not support this proposition.

TEMPORAL AND REGIONAL VARIATIONS IN $\delta^{18}O$ OF THE ROSTRA

The summary of the Middle Jurassic to Early Cretaceous $\delta^{18}O$ values measured by this study in the rostra is given in figure 9. Overall, the trend is an oscillating band with about 3 to 4 permil scatter and the most positive values in the Callovian and Oxfordian. This trend is present regardless of the "degree of preservation," the paleogeographic source of the rostra or the taxonomy.

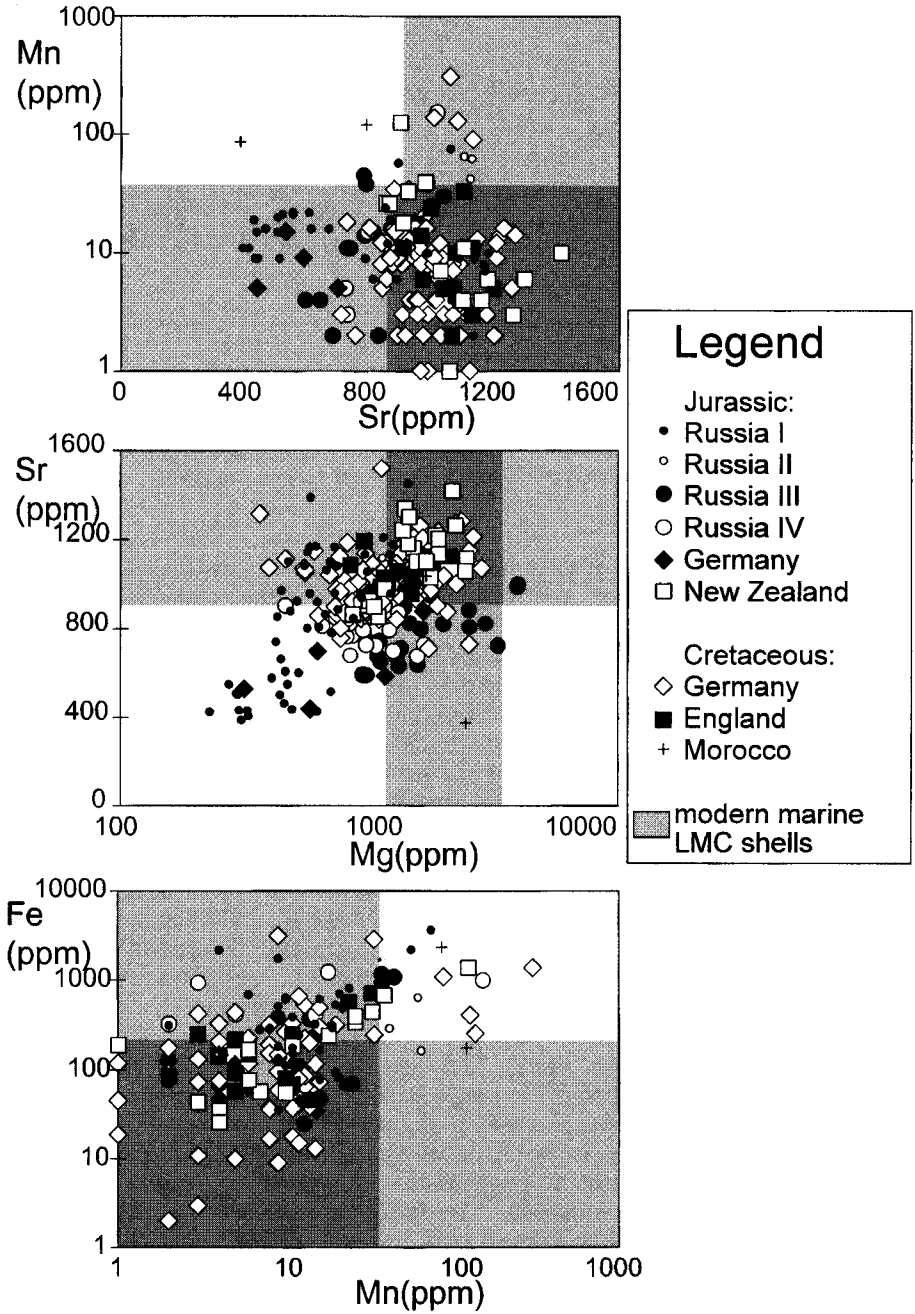

Fig. 6. Scatter diagrams of trace element concentrations in the rostra (App. 2). Russia I-IV as in caption of figure 1. The typical concentrations for modern marine LMC shells from Milliman (1974) and Morrison and Brand (1986).

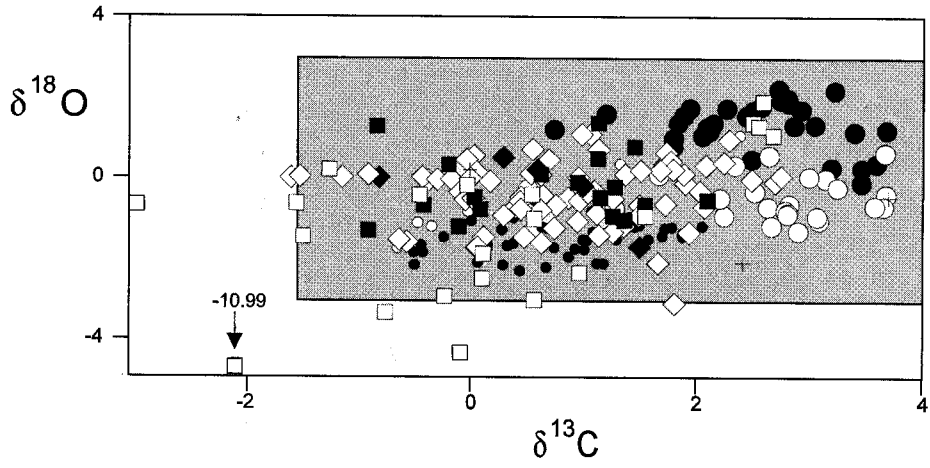

Fig. 7. Scatter diagram of $\delta^{13}C$ and $\delta^{18}O$ in belemnite rostra. Symbols as in figure 6. The shaded box represents values typical of modern LMC brachiopods (Carpenter and Lohmann, 1995).

What is the significance of these long term variations? Are they a primary or a secondary feature of the record, and if the former what is their meaning? Taking into account the well preserved nature of the "laminae pellucidae" in the rostra, the portions exclusively sampled for this study, we believe that the $\delta^{18}O$ and $\delta^{13}C$ trends are essentially primary features of the geologic record. Due to the extinct nature of belemnites, we do not know if isotopic fractionation was associated with the rostra secretion and, therefore, cannot judge how much of the observed scatter could be due to this factor. If of importance, it may result in a shift of the entire pattern, but the internal structure would still be preserved. We therefore suggest that the most likely scenario is that the $\delta^{18}O$ temporal trend and the spread of values reflect the temperature and/or salinity variations of belemnite habitats.

Assuming the $\delta^{18}O$ of Cretaceous and Jurassic seawater to be approx -1 permil SMOW (Shackleton and Kennett, 1975; Pirrie and Marshall, 1990; Ditchfield, Marshall, and Pirrie, 1994) the calculated seawater paleotemperatures appear to decrease from 15 ± 5°C in the Bajocian to 7 ± 4°C at the Callovian/Oxfordian boundary (fig. 9). A warm period during the Tithonian caused a rise of temperatures to 16 ± 5°C, followed by a slight cooling trend to 10 ± 4°C into the Hauterivian, and again a warming to 13 ± 6°C into the Barremian/Aptian (fig. 9). The very large spread of $\delta^{18}O$ values for the Kimmeridgian (New Zealand) and the single positive Tithonian outlier are somewhat enigmatic. The New Zealand samples may perhaps reflect a pronounced warming trend in the course of the Kimmeridgian, but a higher sample density is required to confirm or reject this interference. Are these proposed paleotemperatures reflecting a global trend or are they only regional phenomena? The fact that, for example, the Callovian to Tithonian warming is traceable from Russia to New Zealand (fig. 9), that is from paleolatitudes 42°N to 82°S, suggests that, at least for this portion of the record, the oxygen isotope composition may be recording a global warming, with a sudden temperature jump of ~12°C in the Oxfordian and Kimmeridgian. Geographic temperature difference of 3° to 4°C may, however, account for a considerable proportion of the band width. The general conformity of our paleotemperature trends from northern Europe with those from Svalbard (Ditchfield, 1997) also support our contention that the $\delta^{18}O$ data reflect regional to global trends.

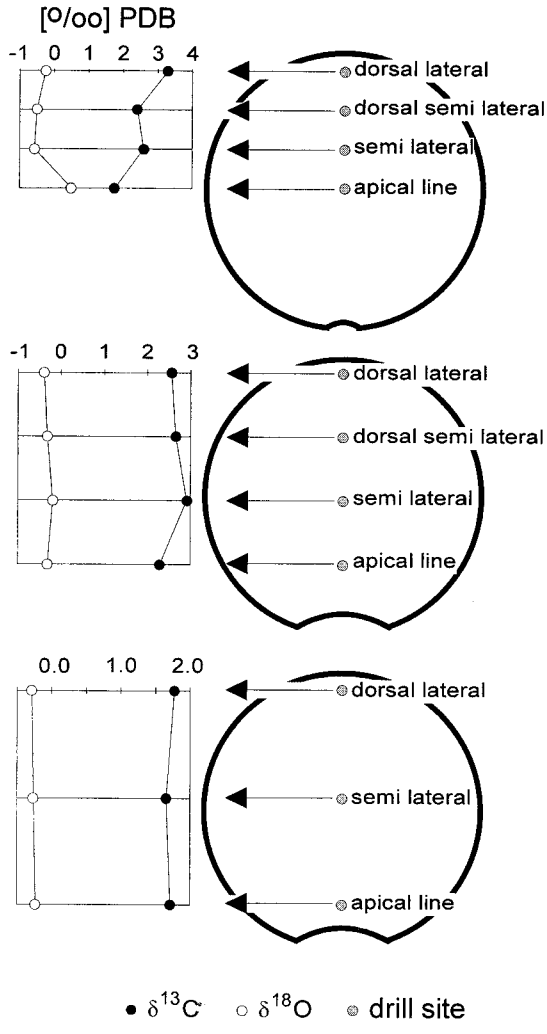

Fig. 8. Variations of $\delta^{13}C$ and $\delta^{18}O$ within single rostrum. The samples were analyzed in the introductory phase of the project, and they are not included in the figures or listed in the appendices; sampled belemnite taxa were (from top to bottom) Megateuthis sp., Pachyteuthis russiensis, and Hibolithes arkelli arkelli.

The above paleotemperature estimates are in general agreement with the paleoclimatic and paleogeographic information for the studied regions. Commencing in the Callovian, the Arctic ocean was connected with the Tethys, and this dominated the paleogeography of the Russian Platform (Dolginow and Kropatschjew, 1994). This Tethyan influence resulted in warming of the waters in the North German-Polish basin and in England, where studies of Anderson and others (1994) suggest Oxfordian/Tithonian paleotemperatures of ~15°C. The calculated late Kimmeridgian paleotemperature for subpolar New Zealand of 18°C appears surprisingly high, but is supported by the estimates of ~18° to 20°C for the coeval Antarctic samples (Ditchfield, Marshall, and Pirrie, 1994), in accord with the proposed general global warming trend in the course of the Kimmeridgian.

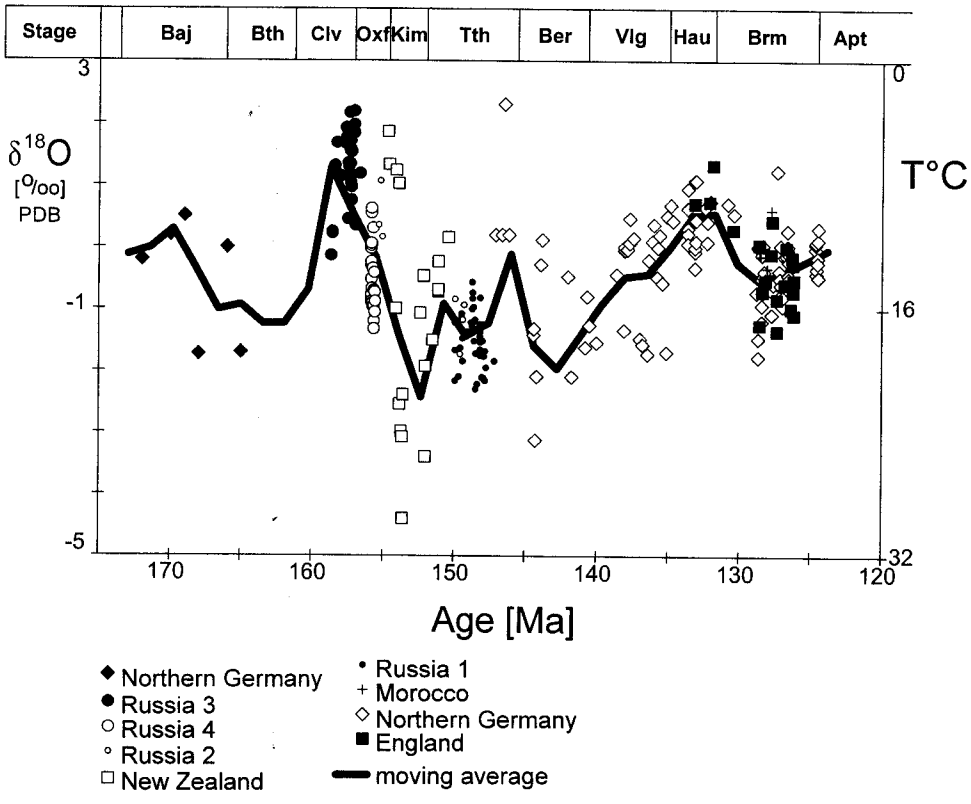

Fig. 9. Geographic variations in $\delta^{18}O$ values for the Late Jurassic and Early Cretaceous belemnite rostra. The window for the running mean (shaded line) is 3.165 Ma. For calculations of paleotemperatures we have assumed $\delta^{18}O$ of seawater to be -1 permil SMOW, utilized the paleotemperature equation of Arthur and Anderson (1983), and taken into account the measured $\delta^{18}O$ ranges of the rostra. See the text for further explanations.

During the Cretaceous, the North German basin was connected mostly to the boreal region via the area of the present North Sea, with intermittent openings to the Tethyan realm via the Paris Basin and possibly over Poland (Mutterlose, 1992 and references therein). As a result, the local Tithonian/Berriasian to Barremian seawater temperatures declined, in accord with our estimates of 18 ± 6°C to 12 ± 2°C.

Another surprising result is the apparently temperate paleotemperature of ~12 ± 4°C off the coast of Morocco (fig. 9). This may reflect the upwelling of a cold Proto-Atlantic water on the north African shelf during the Early Cretaceous (Wiedmann, Butt, and Einsele, 1978), following the opening of the North Atlantic in the later part of this time interval. In general, it appears that latitudinal temperature gradients for the ice cap-free Late Jurassic and Early Cretaceous world (Hallam, 1985; Huber, Hodell, and Hamilton, 1995) were relatively small, and they have been masked by regional difference that may have accounted for a maximum spread of ~3 permil (~12°C) in the observed $\delta^{18}O$ values.

Some of the observed band width for the $\delta^{18}O$ (and $\delta^{13}C$) may result from the existence of short term fluctuations, similar to the Milankovitch frequencies (compare Hagelberg, Bond, and deMenochal, 1994), as recorded in the Quaternary foraminifera.

Unfortunately, and in contrast to the Cenozoic, it is unlikely that the Mesozoic oscillations in the $\delta^{18}O$ and $\delta^{13}C$, even for single sections and with perfectly preserved samples, will ever be resolved to a level comparable to that of the DSDP cores (compare Williams, Lerchie, and Full, 1988). Time resolution on the scale of 10^4 to 10^5 yrs is currently not attainable for the Mesozoic. Therefore, the question to what extent the overall band thickness may reflect high frequency oscillations versus natural variability of the biogenic material remains unsolved.

An alternative interpretation of $\delta^{18}O$ and $\delta^{13}C$ variations could be based on a proposition that these records reflect salinity trends (Sælen, Doyle, and Talbot, 1996). If this were so, the $\delta^{18}O$ and $\delta^{13}C$ would have to co-vary since the influx of low salinity water is depleted in ^{18}O and ^{13}C. This is not the case as seen in figures 7 and 10. Furthermore, the entire range of $\delta^{18}O$ values of about 7 permil would, assuming a $\Delta\delta^{18}O/\Delta S$ gradient of ~0.15 (Geosecs, 1987), require salinity gradient of ~47 permil, an unrealistic proposition in view of the 35 permil salinity of the ocean. Faunal assemblages and sedimentological characteristics of the studied sequences (Cretaceous sections in Mutterlose, 1992 and references therein) also do not support the salinity interpretation.

Composite trends for $\delta^{18}O$ and $\delta^{13}C$ values in belemnites for Jurassic and Early Cretaceous time, based on the present data and the results of Jones, Jenkyns, and Hesselbo (1994) are presented in figure 10. The proposed global or regional anoxic events appear to correlate with ^{18}O depletions (fig. 10). This is the case for the Toarcian (Podlaha, 1995; Jones, Jenkyns, and Hesselbo, 1994), Kimmeridgian, and the Aptian. Of these, the Toarcian and the Aptian events are considered to be of global significance (Schlanger and Jenkyns, 1976; Holser, Magaritz, and Ripperdan, 1996), while the Kimmeridgian is believed to be of regional scope. These ^{18}O depletions may thus indicate that times dominated by warm shallow seas have a propensity for generation of anoxic events, but a causative linkage is difficult to invoke. We shall return to this point after discussing the carbon isotope record.

CARBON ISOTOPE RECORD

The $\delta^{13}C$ of Jurassic-Early Cretaceous belemnites define a secular trend that covaries partially with the oxygen isotopes (fig. 10) and is of comparable band width. The reasons for the width of the band are not entirely clear. One possible alternative could well have been biological fractionation, such as those observed, for example, in corals (Weber and Woodhead, 1970; Swart, 1983) or foraminifera (Wefer, 1985). Unfortunately, belemnites have no living representatives and it is therefore not known whether they may have incorporated carbon into the shells directly from the bicarbonate dissolved in the water or via the food chain and respiratory CO_2. In studies of recent brachiopods, Carpenter and Lohmann (1995) frequently observed a linear covariance, of up to 3 permil, for the $\delta^{13}C$ and $\delta^{18}O$ measured in calcite shells. They attributed this to biological fractionation due to incorporation of respiratory CO_2 into the shell at times of higher temperatures and higher growth rates. Such a linear correlation appears only indistinctly for the belemnite data as a whole (fig. 7), and none was observed within the belemnite rostra itself (fig. 8). For these reasons we do not think that the metabolic effects or kinetic fractionation during hydroxylase of CO_2 (McConnaughey, 1989) were the dominant causes of the observed band width.

Theoretically, the observed long term $\delta^{13}C$ oscillations could reflect the working of the biological pump (Berger and Vincent, 1986) and thus variations in paleoproductivity

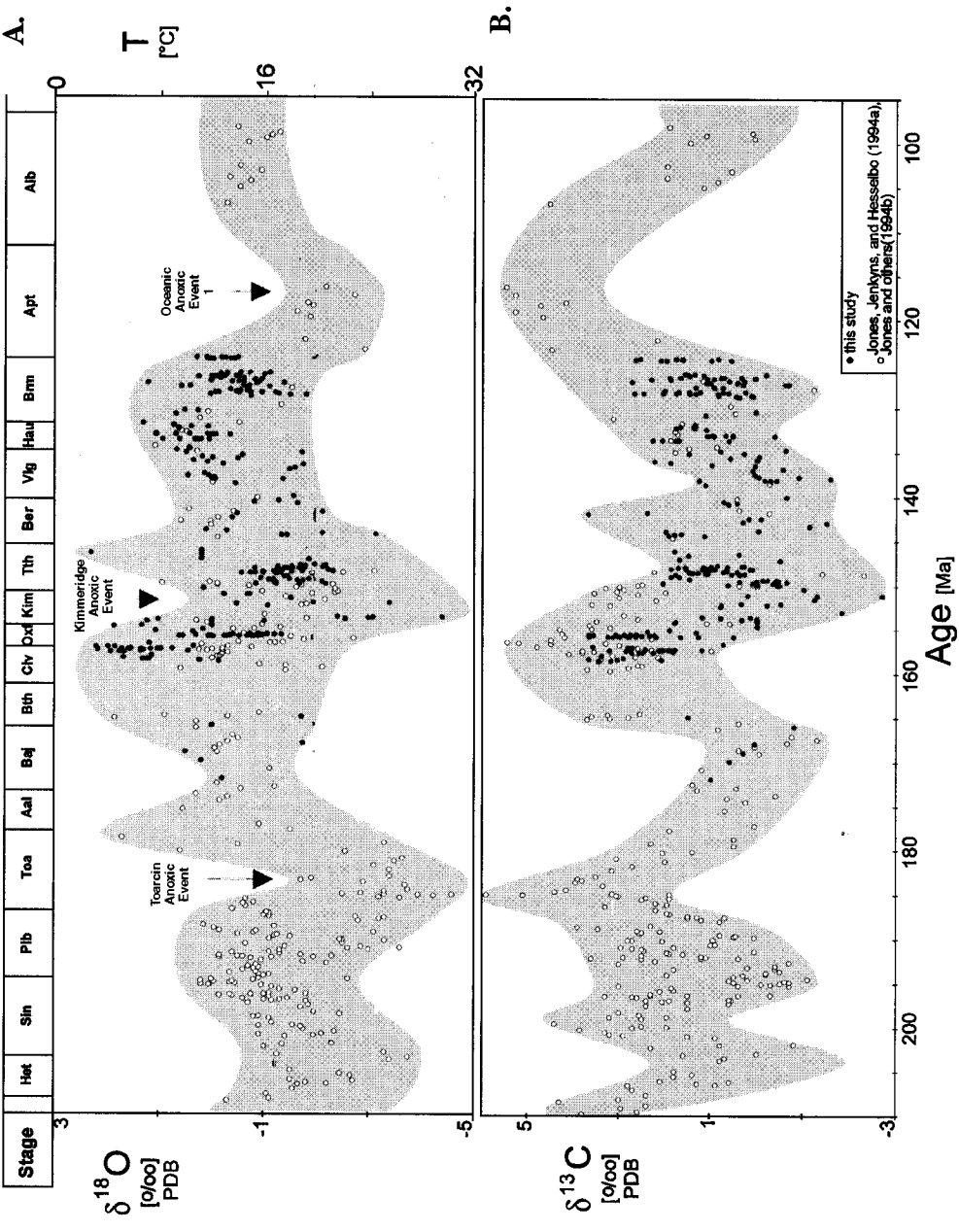

Fig. 10. Variations in $\delta^{18}O$ and $\delta^{13}C$ values of the Jurassic and Early Cretaceous belemnites. The figure includes also the data of Jones, Jenkyns, and Hesselbo (1994) and Jones and others (1994). Extinctions and oceanic anoxic events after Schlanger and Jenkyns (1976) and Holser, Magaritz, and Ripperdan (1996), absolute ages after Harland and others (1990) and Gradstein and others (1994).

within the shallow water column. If so, the enhanced biologic sequestering of the light isotope of carbon during warm times due to surficial productivity should result in ^{13}C enriched ambient dissolved inorganic carbon in surface waters. In this scenario, the warm anoxic events (fig. 10) should be characterized by coincident negative $\delta^{18}O$ and positive $\delta^{13}C$ values (Weissert and Mohr, 1996).

During the Mesozoic, such anoxic events, having the above isotopic signatures, appear to have been coincident with transgressions (Lini, Weissert, and Erba, 1992; Jenkyns, Gale, and Corfield, 1994). In our case, the requisite isotope signatures hold true for the Toarcian and Aptian anoxic events but not for the Kimmeridge. This suggests that their origin is complex and cannot be explained by a single scenario. Furthermore, considering the apparent duration of several million years of these events (fig. 10), they have been likely sustained by external tectonic causes, such as an increased nutrient supply from continents, than by an internal operation of the oceanic biological pump. The latter is essentially self-limiting to time scales of mixing and circulation of oceans, that is to some thousands of years. Because of this complexity, we believe that each oceanic anoxic event has been a result of a combination of its own specific causative factors that will have to be deciphered case by case.

CONCLUSIONS

Optical (cathodoluminescence, SEM) and chemical study of 263 belemnite guards of mid-Jurassic to Lower Cretaceous ages suggest that 90 percent of the specimens have preserved their original texture and chemistry, including the original oxygen and carbon isotopic composition. The remaining 10 percent contained up to 6.8 percent of diagenetic calcite concentrated in domains originally enriched in organic matter ("laminae obscurae"). The post-mortal decay of this organic matter generated secondary porosity that was infilled by calcite cement, thus creating an impression of "growth rings." It is therefore essential to sample only the primary portion of the guard, the so called "laminae pellucidae."

The samples cover a wide variety of paleoclimatic and paleoenvironmental settings (42°N-82°S) and have an average stratigraphic resolution of <1 Ma. Yet, the $\delta^{18}O$ and $\delta^{13}C$ measurements define only flat oscillating bands, with a width of 3 to 4 permil around the near-modern mean values of -1 and $+2$ permil, respectively. In the case of oxygen isotopes, this band likely reflects ambient paleotemperatures that oscillated within $\sim 14 \pm 10$°C range.

The ^{18}O depleted "troughs" in the $\delta^{18}O$ band coincide with the intervals of global and/or regional anoxia, namely the Toarcian, Kimmeridgian, and OAE 1a events. These $\delta^{18}O$ excursions indicate that the events were associated with up to 10°C increases in temperature for the shallow water marine environments, suggesting that they were caused by changing surface temperature gradients and linked to oceanic circulation patterns. Associated with these events are also oscillations in the carbon isotope signal. However, due to the fact that the observed signs of change differ for different events, the causative factors are probably complex and the causative scenario is as yet enigmatic.

ACKNOWLEDGMENTS

The authors thank J. Kaufman and an unknown reviewer for their suggestions and remarks. This research was supported financially by the Leibniz Prize endowment to J. Veizer by the Deutsche Forschungsgemeinschaft (grants Ve112/8-1 and Ve112/11-1). We thank C. Spaeth, R. S. Stevens, and A. B. Challinor for their support with belemnite rostra and local stratigraphic information.

APPENDIX I

Location and stratigraphic data for the samples studied (E, M, L stand for Early, Middle, Late)

No.	Location	Stage	Ammonite Zone	Taxa
	Jurassic:			
1	N. Germany/location not spec.	Dogger δ	?	*Megateuthis* sp.
2-4	"	"	?	"
5	"	Dogger ε	?	*Belemnopsis calloviensis*
6	"	"	?	*Megateuthis* sp.
7	Russia/Peski	Callov (L)	*Peltoceras athleta*	*Pachyteuthis russiensis*
8-9	"	"	"	*Cylindroteuthis beaumonti*
10-14	"	"	"	*Pachyteuthis russiensis*
15-16	"	"	*Quenstedtoceras lamberti*	"
17-18	"	"	"	*Cylindroteuthis puzosiana*
19	"	"	"	*Cylindroteuthis beaumonti*
20	"	"	"	*Cylindroteuthis puzosiana*
21-22	"	"	"	*Pachyteuthis russiensis*
23	"	"	"	*Cylindroteuthis puzosiana*
24	"	"	"	*Pachyteuthis russiensis*
25-26	"	"	"	*Cylindroteuthis puzosiana*
27-28	"	"	"	*Hibolithes* sp.
29-30	"	"	"	*Pachyteuthis russiensis*
31	"	"	"	"
32-34	"	"	*Q. lamberti/mariae*	"
35	"	Callov/Oxford	*Quenstedtoceras mariae*	*Cylindroteuthis beaumonti*
36	"	Oxford (E)	*Cardioceras cordatum*	"
37-52	Russia/Jaroslawskaja	Oxford (L)	*Amoeboceras alternoides*	*Pachyteuthis russiensis*
53	"	"	"	*Hibolithes* sp.
54-61	"	"	"	*Pachyteuthis russiensis*
62	Russia/Voskresjensk N7-2bis	"	"	*Acroteuthis* sp.
63-64	"	"	*Amoeboceras ravni*	"
65	New Zealand/Kawhia Harbour	Oxford	*Amoeboceras rosenkrantzi*	*Belemnopsis annae*
66	"	Kimmeridge	*Pictonia baylei*	"
67	"	"	*Rasenia cymodoce*	"
68	"	"	"	*Belemnopsis keari*
69-71	"	"	"	*Belemnopsis maccrawi*
72	"	"	"	*Belemnopsis keari*
73-74	"	"	*Aulacostephanus mutabilis*	"
75	"	"	*Aulacostephanus eudoxus*	*Dicoelites kowhaiensis*
76-78	"	"	*Aulacostephanus autissiodorensis*	*Belemnopsis aucklandica trechmanni*
79	"	Kimm./Tithon	*Pectinatites elegans*	*Hibolithes spathi*
80	"	"	"	*Belemnopsis spathi*
81	"	Tithon	*Pectinatites scitulus*	*Hibolithes arkelli arkelli*
82	"	"	*Pectinatites wheatleyensis*	"
83	"	"	"	*Hibolithes marwicki marwicki*
84	"	"	"	*Hibolithes arkelli arkelli*
85	"	"	*Pectinatites pectinatus*	*Belemnopsis aucklandica aucklandica*
86-91	Russia/Voskresjensk N9-2bis	Volgium	*Virgatites virgatus*	*Pachyteuthis panderiana*
92	Russia/Voskresjensk N7-2bis	"	"	*Cylindroteuthis volgensis*
93	Russia/Voskresjensk N9-2bis	"	"	"
94	Russia/Voskresjensk N7-2bis	"	"	"
95-96	Russia/Voskresjensk N9-2bis	"	"	*Cylindroteuthis magnifica*
97	Russia/Voskresjensk N7-2bis	"	"	*Pachyteuthis panderiana*
98	Russia/Voskresjensk N9-2bis	"	"	*Pachyteuthis russiensis*
99	Russia/Voskresjensk N7-2bis	"	"	*Cylindroteuthis volgensis*
100	Russia/Voskresjensk N9-2bis	"	"	*Pachyteuthis russiensis*
101	Russia/Voskresjensk N7-2bis	"	"	*Cylindroteuthis volgensis*
102-103	Russia/Voskresjensk N9-2bis	"	"	*Pachyteuthis russiensis*
104	Russia/Voskresjensk N7-2bis	"	"	*Cylindroteuthis volgensis*
105-121	Russia/Voskresjensk N9-2bis	"	*Epivirgatites nikitini*	"
122-129	"	"	*Kaspurites fulgens*	*Pachyteuthis russiensis*
130-139	"	"	"	*Cylindroteuthis volgensis*
140	N. Germany/location not spec.	Tithon	*Paracraspedites oppressus*	
141-142	"	"	*Subcraspedites primitivus*	
143	"	"	*Subcraspedites preplicomphalus*	
	Cretaceous			
144-147	N. Germany/location not spec.	Berrias	*Surites icenii*	
148-149	"	"	"	
150-152	"	Valangin (E)	*Platylenticeras robustum*	
153-156	"		*Platylenticeras involutum*	
157-159	"	"	*Polyptiches brancoi*	
160	"	"	*Polyptychites sphaeroidalis*	
161-162	"	Valangin (L)	*Dichotomites biscissoides*	
163-166	"	"	*Dichotomites bidochotomus*	
167-169	"	"	*tuberculata*	*Acroteuthis paracmonoides arctica*
170	N. Germany/Diepenau	"	"	*Acroteuthis paracmonoides arctica*
171-172	N. Germany/location not spec.	"	"	
173-174	N. Germany/Engelbostel	Hauterive (E)	*Endemoceras amblygonium*	*Acroteuthis paracmonoides arctica*
175-180	N. Germany/Moorberg	Hauterive	*Simbirskites inversum*	*Hibolithes jaculoides*
181-188	"	"	*Simbirskites sp.=gottschei*	"
189	N. Germany/Frielingen	Hauterive (L)	*Simbirskites discofalcatum*	*Acrotheutis stolleyi*
190-191	N. Germany/Gott	"	"	
192	England/Speeton	"	"	*variabilis ?*

193	N. Germany/Frielingen	"	"	*Acrotheutis stolleyi*
194	England/Speeton	Barrême (E)	*Hoplocrioceras rarocinctum*	*Praeoxyteuthis pugio*
195	N. Germany/Gott	"	"	*Acrotheutis stolleyi*
196	England/Speeton	"	"	*Praeoxyteuthis pugio*
197	N. Germany/Gott	"	"	*Acrotheutis stolleyi*
198	"	"	*Hoplocrioceras fissicostatum*	*Hibolithes minutus*
199	Morocco/Agadir	"	"	*Duvalia* sp.
200-201	N. Germany/Gott	"	"	*Aulacoteuthus speetonensis*
202	England/Speeton	"	"	*Hibolithes minutus*
203	"	"	"	*Aulacoteuthis* sp.
204	N. Germany/Gott	"	"	*Aulacotheutis absolutiformis*
205	"	"	"	*Hibolithes minutus*
206-207	"	"	"	*Aulacotheutis absolutiformis*
208	"	"	"	*Hibolithes minutus*
209	England/Speeton	"	"	*Aulacoteuthis* sp.
210	N. Germany/Gott	"	"	*Hibolithes minutus*
211	Morocco/Agadir	"	"	*Duvalia* sp.
212-213	N. Germany/Gott	"	"	*Aulacotheutis absolutiformis*
214	Morocco/Agadir	"	"	*Duvalia* sp.
215-216	N. Germany/Gott	"	"	*Aulacotheutis ascendus*
217-218	"	"	"	*Hibolithes minutus*
219	England/Speeton	"	"	*Aulacoteuthis* sp.
220	N. Germany/Gott	"	"	*Aulacotheutis descendens*
221-222	Morocco/Agadir	"	"	*Hibolithes* sp.
223-224	N. Germany/Gott	"	"	*Aulacotheutis descendens*
225	England/Speeton	"	"	*Aulacoteuthis* sp.
226	N. Germany/Gott	"	"	*Aulacotheutis descendens*
227-228	England/Speeton	Barrême (M)	*Paracrioceras elegans*	*Oxyteuthis brunsvicensis*
229	"	Barrême (L)	"	"
230	N. Germany/Gott	"	"	"
231-232	"	"	"	*Oxytheutis oxys?*
233-234	"	"	"	*Oxytheutis brunsvicensis*
235-237	"	"	*Paracrioceras denckmanni*	
238	England/Speeton	"	"	
239-243	N. Germany/Gott	"	*Ancyloceras innexum*	
244-246	"	"	*Simancyloceras stolleyi*	
247	"	"	"	*Oxytheutis brunsvicensis*
248-253	England/Speeton	"	*Parancycloceras bidentatum*	*Praeoxyteuthis jasikofiana ?*
254-258	N. Germany/Gott	"	"	
259	"	"	"	*Oxytheutis depressa*
260-261	"	"	"	
262-263	"	Apt (L)	*Parahoplites nutfieldiensis*	

Appendix II

Sample age and geochemistry

1	GER08SC	172.00	174.16	575	434	5	96	1.00	-0.20		
2	GER02SC	170.00	172.18	313	526	15	35	0.60	0.20		
3	GER03SC	169.00	171.19	1150	583	9	135	0.30	0.50		
4	GER07SC	168.00	170.20	1453	949	4	46	0.06	-1.73		
5	GER01SC	166.00	168.21	615	694	5	114	-0.80	0.00		
6	GER04SC	165.00	167.22	1647	876	12	42	1.50	-1.70		
7	47	158.67	161.27	1365	896	13	25	3.46	-0.13	0.706726	7
8	48	158.59	161.17	872	784	38	916	3.20	0.25		
9	49	"	"	892	777	45	1081	3.46	0.23		
10	50	158.47	161.03	1251	1033	30	0	2.09	1.24		
11	51	"	"	729	865	16	48	3.05	1.31	0.706720	7
12	52	158.43	160.98	981	732	11	62	3.68	1.19	0.706755	11
13	53	158.31	160.84	1746	948	12	107	2.93	1.68	0.706746	7
14	54	158.05	160.53	923	780	14	364	3.40	1.14		
15	64	157.67	160.08	1590	800	0	44	2.50	1.66	0.706794	31
16	65	"	"	1087	745	0	115	2.75	1.92	0.706733	7
17	57	157.65	160.05	2495	883	9	375	2.26	1.72		
18	58	"	"	1675	719	0	261	2.57	1.76		
19	55	157.53	159.91	1296	982	38	1161	2.49	0.45		
20	56	"	"	2508	809	15	231	1.84	1.35		
21	69	157.47	159.84	1963	822	0	26	2.86	1.30	0.706719	8
22	68	157.42	159.78	1329	709	0	0	3.23	2.17	0.706776	11
23	59	157.38	159.73	1274	674	0	732	2.15	1.34		
24	66	"	"	1304	630	0	71	1.89	1.55	0.706739	9
25	60	157.35	159.70	1095	650	0	0	1.20	1.58	0.706730	7
26	61	"	"	947	758	0	260	1.94	1.71		
27	71	157.33	159.67	3269	723	11	179	2.05	1.03		
28	71-II	"	"	2905	823	0	0	2.11	1.16		
29	67	157.29	159.63	3935	998	25	69	1.79	0.75		
30	67-II	"	"	3907	989	9	0	1.80	0.97		
31	73	157.27	159.60	964	589	4	28	2.44	1.54	0.706726	7
32	70	157.10	159.40	1550	636	4	69	2.82	1.84	0.706727	7
33	72	"	"	1444	825	2	77	2.73	2.19	0.706737	7
34	74	"	"	1070	676	2	126	2.80	1.97	0.706738	7

Appendix II

Sample age and geochemistry

35	63	157.00	159.18	895	828	0	36	3.59	0.35		
36	62	156.68	158.47	930	591	0	0	0.74	1.19	0.706725	8
37	97	155.90	156.74	1530	677	0	147	3.15	-0.02	0.706788	8
38	98	155.86	156.65	747	865	0	437	2.64	0.55		
39	100	155.86	156.65	836	767	0	456	2.79	-0.81		
40	101	"	"	927	793	0	223	3.00	0.03		
41	102	"	"	793	764	0	546	1.28	-0.76		
42	103	"	"	816	821	0	19	0.52	-0.29	0.706776	8
43	104	"	"	634	812	0	198	2.21	-0.51	0.706818	21
44	105	"	"	452	903	0	284	3.67	0.63		
45	106	"	"	948	907	0	107	2.81	-0.88	0.706806	10
46	107	155.86	156.65	1185	794	15	409	3.25	-0.24		
47	108	"	"	1224	700	0	324	1.67	0.06		
48	99	155.83	156.60	1416	1016	153	1012	2.82	-0.66		
49	113	155.79	156.51	793	857	0	28	2.81	-0.90	0.706769	8
50	112	155.77	156.46	1043	722	5	420	2.52	-0.35		
51	91	155.75	156.41	821	679	0	0	2.34	0.31	0.706809	8
52	109	155.75	156.41	836	866	0	127	3.07	-0.96	0.706778	7
53	93	155.68	156.27	953	727	0	138	2.25	-0.94	0.706831	32
54	111	155.68	156.27	718	850	0	186	3.58	-0.69	0.706785	7
55	95	155.66	156.23	879	883	18	1245	2.67	-1.19		
56	96	155.66	156.22	1287	874	0	396	2.90	-1.32		
57	110	155.66	156.22	1132	905	2	326	3.68	-0.40		
58	110-II	"	"	937	942	0	0	3.66	-0.71		
59	94	155.64	156.17	1636	728	3	941	2.63	-0.72		
60	90	155.62	156.13	813	887	0	328	3.09	-1.05		
61	92	155.60	156.08	798	841	0	125	2.76	-0.87	0.706797	6
62	44	155.36	155.56	1848	1098	65	163	1.33	0.36		
63	45	155.23	155.27	1193	1124	62	640	2.39	1.07		
64	46	155.10	154.98	1124	1119	42	289	1.91	0.17		
65	NZ01ABC	154.70	154.09	1390	1331	0	28	2.82	1.86	0.706727	7
66	NZ02ABC	154.62	153.99	1843	1211	0	132	2.73	1.33	0.706727	6
67	NZ03ABC	154.13	153.36	1503	1155	4	35	2.78	1.24	0.706604	8
68	NZ16SGR	"	"	2453	1110	0	21	1.78	-0.99	0.706781	7
69	NZ04ABC	153.96	153.13	1421	1174	6	165	2.91	1.02	0.706685	7
70	NZ05ABC	153.86	153.00	2430	1053	1	186	0.34	-2.54	0.706737	7
71	NZ06ABC	153.75	152.86	2154	1410	10	55	0.01	-2.98	0.706755	8
72	NZ17SGR	153.68	152.77	1900	1131	0	114	0.80	-3.07	0.706772	8
73	NZ07ABC	153.61	152.68	1542	1095	4	26	1.20	-2.39	0.706763	8
74	NZ18SGR	"	"	1689	1098	11	181	0.15	-4.40	0.706746	8
75	NZ08ABC	153.01	151.89	1085	849	26	336	-1.84	-10.99	0.706611	7
76	NZ09ABC	152.41	151.11	1892	1197	0	28	0.80	-1.06	0.706839	7
77	NZ10ABC	152.20	150.83	1753	1023	7	57	-0.21	-0.47	0.706872	7
78	NZ19SGR	"	"	1362	1235	0	43	0.78	-0.46	0.706862	8
79	NZ11ABC	152.05	150.65	1443	1294	6	76	0.35	-1.93	0.706871	8
80	NZ20SGR	152.05	150.63	923	902	18	234	-0.51	-3.39	0.706867	7
81	NZ12ABC	151.54	150.14	990	918	33	436	-1.24	-1.50	0.706925	7
82	NZ13ABC	151.13	149.73	1041	894	125	1365	-2.71	-0.71	0.706952	7
83	NZ14ABC	"	"	2212	1257	3	43	0.21	-0.23	0.706951	7
84	NZ21SGR	"	"	1145	974	39	674	-1.30	-0.68	0.706956	7
85	NZ15ABC	150.44	149.04	855	859	26	390	-1.01	0.16	0.707033	7
86	1	149.96	148.56	688	1101	0	688	0.64	-1.22	0.707089	9
87	1-II	"	"	739	1083	0	111				
88	2	"	"	1240	1179	10	633	-0.43	-1.67		
89	2-II	"	"	1344	984	10	607				
90	3	"	"	1211	1131	2	310	-0.49	-2.16	0.707058	9
91	3-II	149.96	148.56	1213	959	0	364				
92	41	149.95	148.55	227	424	19	0	-0.01	-0.83	0.707105	24
93	9-II	149.82	148.42	509	925	0	217	2.05	-1.19		
94	42	149.75	148.35	304	388	11	112	-0.33	-1.21	0.707111	11
95	4	149.70	148.30	1212	1133	9	1752	0.07	-2.09		
96	4-II	"	"	1399	1058	4	2183				
97	38	149.60	148.20	613	427	9	0	-0.64	-1.73	0.707071	7
98	5	149.57	148.17	1430	1452	0	17	0.39	-1.63	0.707066	8
99	40	149.50	148.10	293	501	20	93	-0.46	-1.11		
100	6	149.49	148.09	1135	1208	0	11	0.01	-1.07	0.707070	7
101	39	149.42	148.02	297	432	15	324	-0.12	-1.17		
102	7	149.41	148.01	719	1167	7	277	-0.41	-1.84	0.707079	7
103	7-II	"	"	571	958	0	0	-0.23	-1.47		
104	43	149.33	147.93	954	1134	11	174	1.48	-0.93	0.707072	8
105	8	149.09	147.69	606	1168	0	27	1.70	-1.43	0.707075	8
106	8-II	"	"	613	921	0	184	1.88	-1.37		
107	9	148.82	147.42	441	973	0	51	1.79	-1.22	0.707069	8
108	10	148.75	147.38	558	802	0	191	0.39	-1.00	0.707067	8
109	11	148.74	147.34	698	782	9	505	0.57	-0.56		
110	12	148.72	147.32	621	807	6	688	0.28	-1.29	0.707100	8
111	13	148.70	147.30	573	1165	8	288	1.13	-0.73		
112	13-II	"	"	576	1388	0	0	1.08	-0.82		
113	14	148.64	147.24	478	880	6	57	1.41	-0.97	0.707073	8
114	15	148.58	147.18	561	1143	11	385	1.30	-1.52		
115	15-II	"	"	469	1104	0	0	1.45	-1.21		
116	16	148.55	147.15	545	1083	9	128	1.50	-1.18	0.707106	15
117	17	148.49	147.09	719	961	19	292	0.44	-2.30		
118	18	"	"	924	940	20	523	0.74	-1.72		
119	19	148.46	147.06	424	854	12	237	1.09	-1.33		
120	20	148.38	146.98	658	864	19	310	0.67	-2.22		

121	21	148.19	146.79	667	1063	10	111	1.88	-1.45	0.707123	10
122	22	148.18	146.78	743	888	57	2202	0.93	-1.76		
123	22-II	"	"	975	1056	75	3662	1.00	-1.52		
124	23	"	"	695	515	21	698	0.11	-1.76		
125	24	"	"	859	846	24	815	1.19	-1.38		
126	25	"	"	516	600	22	479	0.68	-1.25		
127	26	"	"	438	664	16	164	1.04	-1.53	0.707079	7
128	27	"	"	418	741	11	154	1.56	-0.81	0.707073	7
129	28	"	"	324	407	11	122	0.16	-1.66	0.707078	8
130	30	148.06	146.66	321	429	9	122	1.12	-2.11	0.707072	7
131	37-2	148.02	146.62	271	549	22	66	1.72	-1.25		
132	37-2-II	"	"	731	1080	0	0	1.58	-1.52		
133	31	147.95	146.55	435	500	15	316	1.18	-2.12		
134	32	147.91	146.51	290	506	9	180	1.01	-1.77	0.707069	9
135	33	"	"	403	576	9	133	0.65	-1.69	0.707062	8
136	34	147.83	146.43	465	549	21	80	0.29	-2.16		
137	35	"	"	455	607	16	77	0.34	-1.68	0.707074	8
138	29	147.75	146.35	451	462	16	612	0.87	-1.95		
139	36	147.19	145.79	485	435	9	36	-0.50	-1.84	0.707114	14
140	252	147.10	145.70	1027	1027	2	176	1.70	0.20		
141	251	146.65	145.25	1385	1105	0	128	1.50	0.20		
142	248	146.50	145.10	1068	958	0	301	0.40	2.30		
143	249	146.20	144.80	961	928	4	326	1.80	0.20		
144	247	144.43	142.65	813	905	3	74	1.15	-1.42		
145	246	144.42	142.64	2342	1277	0	378	1.93	-1.32		
146	245	144.30	142.47	1114	1514	0	103	1.81	-3.12		
147	244	144.21	142.34	1368	1122	0	110	1.66	-2.10		
148	243	140.82	137.46	686	1039	3	0	0.64	-1.62		
149	250	140.70	137.29	919	1009	4	0	0.45	-0.79		
150	242	140.54	137.04	546	1047	0	85	0.74	-1.26		
151	241	140.03	136.57	360	1309	0	0	-0.63	-1.54		
152	291	138.64	135.31	456	1111	3	130	1.14	-0.44	0.707213	8
153	240	138.12	134.83	540	1068	3	43	1.28	-1.34		
154	292	138.11	134.83	598	1144	0	89	-0.28	-0.05	0.707211	7
155	293	"	"	393	1071	0	0	-0.15	-0.04	0.707234	5
156	302	"	"	758	1119	0	49	-0.41	0.01	0.707225	6
157	294	137.91	134.65	1014	1090	2	0	-1.58	-0.03	0.707221	7
158	295	137.74	134.49	792	1013	4	205	-0.02	0.47	0.707226	7
159	301	"	"	546	1059	5	0	-0.90	0.07	0.707234	7
160	296	137.49	134.26	809	1181	0	0	0.07	0.15	0.707221	7
161	239	137.02	133.84	731	973	20	309	0.11	-1.47		
162	238	136.84	133.67	941	992	8	189	-0.55	-1.57		
163	237	136.48	133.35	792	927	13	525	0.06	-1.73		
164	236	136.43	133.30	862	946	10	258	1.00	-0.20		
165	235	136.17	133.06	1468	1199	2	91	1.90	0.10		
166	234	136.05	132.96	761	754	2	2	2.25	0.37		
167	299	135.83	132.75	1437	1208	9	153	0.02	-0.48		
168	233	135.77	132.70	1220	987	0	317	0.00	0.00		
169	232	135.64	132.58	866	902	8	313	0.60	0.20		
170	300	135.44	132.40	1374	1177	3	11	-0.03	-0.57		
171	231	135.15	132.14	1485	1113	0	129	1.50	-1.70		
172	230	135.11	132.10	1303	946	0	117	0.30	0.50		
173	297	134.88	131.80	1396	1003	0	214	0.81	0.68	0.707317	6
174	298	134.72	131.53	1319	1039	0	52	-0.60	0.43	0.707274	7
175	217	133.68	129.80	1233	988	0	206	1.72	0.34		
176	218	"	"	1032	1028	2	91	2.29	0.94		
177	219	133.68	129.80	1500	1143	0	122	2.09	0.31		
178	220	"	"	760	799	16	491	1.74	0.63		
179	221	"	"	1082	947	4	146	1.79	0.22		
180	222	"	"	1481	1122	1	46	0.63	0.07		
181	223	133.15	128.92	1151	987	1	119	-0.36	-0.06		
182	224	"	"	976	858	11	326	0.96	0.00		
183	224-II	"	"					0.56	0.70		
184	225	"	"	1302	1051	8	152	1.07	1.07		
185	226	133.15	128.92	831	981	16	299	1.10	-0.33		
186	227	133.08	128.80	983	941	13	223	0.99	1.08		
187	228	"	"	1323	1127	0	61	0.54	0.10		
188	229	"	"	972	955	4	75	0.70	0.44		
189	402	132.42	127.70	1549	1220	14	197	1.12	0.65		
190	253	132.29	127.48	1110	1048	0	23	1.78	0.41	0.707393	7
191	253-II	"	"	1047	1025	12	661	1.38	0.09		
192	200	132.13	127.22	1652	1126	3	249	1.69	0.73	0.707369	7
193	401	132.08	127.13	1588	1257	5	431	1.40	0.74		
194	201	131.87	126.90	830	1087	4	143	1.37	1.32	0.707352	7
195	400 a	130.84	126.07	984	986	3	422	1.14	0.70		
196	202	130.47	125.78	1555	1073	10	81	0.05	0.28	0.707359	6
197	400 i	130.41	125.73	1006	853	0	28	0.04	0.54		
198	267	128.82	124.45	2221	1267	14	39	0.41	-0.72	0.707370	8
199	404 a	128.72	124.38	1624	1081	128	404	-1.13	0.02		
200	254	128.69	124.35	1630	1201	0	226	0.48	-1.47	0.707388	7
201	254-II	"	"	1280	1087	8	0	0.11	-1.78		
202	203	128.62	124.30	1105	991	24	570	0.86	0.04		
203	204	128.58	124.26	946	1194	5	216	0.14	-1.26		
204	262	128.44	124.15	840	894	9	3130	0.87	-0.50		
205	261	128.43	124.14	2505	1146	13	65	1.36	-1.19	0.707384	6
206	263	"	"	871	888	2	0	1.49	-0.93	0.707353	7

207	264	"	"	734	861	9	9	2.49	-0.04	0.707448	10
208	265	"	"	1796	991	7	0	2.70	-0.11	0.707437	11
209	205	128.38	124.10	1739	1066	5	93	1.78	-0.70	0.707423	19
210	259	128.38	124.10	1250	1065	8	38	2.07	-0.72	0.707378	7
211	404 m	128.38	124.10	1491	1006	138	252	-1.50	0.04		
212	257	128.33	124.06	2528	1094	11	18	0.65	-0.45	0.707376	11
213	257-II	"	"	849	920	13	86				
214	404 i	128.28	124.03	2480	1105	0	169	-0.08	-0.38	0.707374	7
215	255	128.26	124.01	2809	1068	7	0	1.50	-0.68	0.707369	2
216	256	128.24	123.99	1204	960	11	37	1.73	-0.65	0.707373	7
217	266	128.22	123.98	1887	1230	16	0	0.76	-0.69	0.707385	7
218	260	128.21	123.97	1596	953	3	3	1.27	-0.52	0.707407	12
219	206	128.18	123.94	2083	1127	11	248	0.28	-0.53		
220	258	128.04	123.87	1758	971	2	0	2.03	-0.33	0.707384	8
221	403	127.79	123.63	1892	1016	0	13	0.32	0.60	0.707316	7
222	403-II	127.79	123.63					0.19	-0.10		
223	269	127.76	123.61	1001	915	2	0	0.95	-1.08	0.707391	10
224	270	127.73	123.58	986	1022	6	117	0.76	-0.69	0.707386	8
225	207	127.71	123.57	1468	961	14	46	1.36	0.43	0.707399	8
226	268	127.64	123.51	992	924	34	245	0.97	-0.59		
227	208	127.38	123.30	1482	1033	5	59	0.33	-0.83	0.707365	7
228	209	127.35	123.28	1794	1099	33	710	-0.67	-1.35		
229	303	"	"	2611	1208	12	15	-0.59	1.23	0.707375	7
230	271	127.22	123.17	1627	1125	3	3	1.04	-0.37	0.707361	7
231	274	127.20	123.16	892	853	12	79	1.12	-0.89	0.707388	6
232	272	127.19	123.15	760	963	1	19	0.46	-0.50	0.707422	15
233	276	127.13	123.10	721	896	15	116	2.75	0.04	0.707388	9
234	277	127.12	123.10	2226	997	10	0	0.44	-0.59	0.707389	8
235	275	126.97	122.98	1515	965	8	17	0.30	-0.94	0.707418	19
236	275-II	"	"	1980	1033	9	59	0.63	-0.80		
237	273	126.83	122.86	1117	919	11	0	1.91	-0.14	0.707367	8
238	210	126.82	122.86	951	944	0	183	2.33	-0.59	0.707426	16
239	284	126.73	122.78					0.96	0.00	0.707351	7
240	284-II	"	"	2502	726	18	0	1.11	-0.12		
241	283	126.66	122.72	2041	873	8	0	0.07	-0.03	0.707361	7
242	283-II	"	"	1867	900	0	0	0.05	0.27		
243	282	126.63	122.71	1276	838	12	0	1.92	0.02	0.707352	8
244	281	126.61	122.69	1087	836	8	0	1.70	-0.07	0.707339	7
245	280	126.59	122.67	917	841	5	10	0.82	-0.44	0.707361	7
246	279	126.57	122.65	1017	886	9	0	0.74	-0.22	0.707359	8
247	278	126.56	122.65	918	1004	8	36	0.36	-0.50	0.707370	8
248	211	126.40	122.52	1031	967	6	150	1.49	-0.99		
249	212	126.32	122.46	951	906	11	69	1.19	-0.15		
250	213	126.27	122.41	1135	1033	5	58	1.51	-0.27		
251	214	126.23	122.38	1293	1061	2	87	-0.18	-0.71		
252	215	126.20	122.36	1465	1038	0	69	1.38	-0.53		
253	216	126.19	122.35	1184	1006	0	117	1.60	-1.09		
254	287	124.67	121.13	897	1008	9	96	2.12	-0.01	0.707316	7
255	287-II	"	"	900	879	16	73	2.00	0.06		
256	285	124.62	121.10	960	1132	89	1093	1.02	0.09		
257	285-II	"	"	934	1059	305	1367	0.59	-0.42		
258	286	124.62	121.09	619	855	6	224	2.67	-0.34		
259	288	124.53	121.02	957	879	34	2843	1.66	-0.16		
260	288-II	"	"	786	866	9	147	1.64	-0.24		
261	304	124.51	121.01	1526	931	0	0	1.79	0.12	0.707316	7
262	289	124.49	120.99	959	881	15	13	0.87	-0.48	0.707132	11
263	290	"	"	1721	708	3	0	2.57	0.31	0.707129	8

References

Anderson, T. F., Popp, B. N., Williams, A. C., Ho, L.-Z., and Hudson, J. D., 1994, The stable isotopic records of fossils from the Peterborough Member, Oxford Clay Formation (Jurassic), U.K.: palaeoenvironmental implications: Journal of the Geological Society of London, v. 151, p. 125–138.

Arthur, M. A., and Anderson, T. F., 1983, Stable isotopes of oxygen and carbon and their application to sedimentological and paleoenvironmental problems, *in* Arthur, M. A., Anderson, T. F., Kaplan, I. R., Veizer, J., and Land, L. S., editors, Stable isotopes in sedimentary geochemistry: Society of Economic Paleontologists and Mineralogists Short Course, v. 10, p. 1–151.

Arthur, M. A., Dean, W. E., and Pratt, L. M., 1988, Geochemical and climatic effects of increased marine organic carbon burial at the Cenomanian/Turonian boundary: Nature, v. 335, p. 714–717.

Banner, J. L., 1995, Application of the trace element and isotope geochemistry of strontium to studies of carbonate diagenesis: Sedimentology, v. 42, p. 805–824.

Berger, W. H., and Vincent, E., 1986, Deep-sea carbonates: reading the carbon isotope signal: Geologische Rundschau, v. 75, p. 249–269.

Bøggild, O. B., 1930, The shell structure of the mollusks: Kongelige Danske Videnskabernes Selska, Naturvidenskabe Mathematiske Avdelningen, 9. Raekke Kopenhagen, v. 2, p. 258–325.

Bowen, R. N. C., 1966, Paleotemperature analysis: Amsterdam, Elsevier, 265 p.

Brand, U., 1989, Biogeochemistry of Paleozoic North American brachiopods and secular variation of seawater composition: Biogeochemistry, v. 7, p. 159–193.

Brand, U., and Veizer, J., 1980, Chemical diagenesis of a multicomponent carbonate system.–1: Trace elements: Journal of Sedimentary Petrology, v. 50, p. 1219–1236.
Brennecke, J. C., 1977, A comparison of the stable oxygen and carbon isotope composition of the Early Cretaceous and Late Jurassic carbonates from DSDP sites 105 and 367: Initial Reports Deep Sea Drilling Project, v. 41, p. 937–955.
Bruckschen, P., and Veizer, J., 1997, Oxygen and carbon isotopic composition of Dinantian brachiopods: implications for Lower Carboniferous sea water of western Europe: Palaeogeography, Palaeoclimatology, Palaeoecology, v. 132, p. 243–264.
Bruhn, F., Bruckschen, P., Richter, D. K., Meijer, J., Stephan, A., and Veizer, J., 1995, Diagenetic history of sedimentary carbonates: constraints from combined cathodoluminescence and trace element analyses by micro-PIXE: Nuclear Instruments and Methods in Physics Research B, v. 104, p. 409–414.
Carpenter, S. J., and Lohmann, K. C., 1995, $\delta^{18}O$ and $\delta^{13}C$ values of modern brachiopod shells: Geochimica et Cosmochimica Acta, v. 59, p. 3749–3764.
Coleman, M. L., Walsh, J. N., and Benmore, R. A., 1989, Determination of both chemical and stable isotope composition in milligram-size carbonate samples: Sedimentary Geology, v. 65, p. 233–238.
Corfield, R. M., 1995, An introduction to the techniques, limitations and landmarks of carbonate oxygen paleothermometry: Geological Society of America Special Publication, v. 46, p. 27–43.
Degens, E. T., and Epstein, S., 1962, Relationship between O^{18}/O^{16} ratios in coexisting carbonates, cherts and diatomites: American Association of Petroleum Geologists Bulletin, v. 46, p. 534–542.
Ditchfield, P. W., 1997, High northern paleolatitude Jurassic-Cretaceous paleotemperature variation: new data from Kong Karls Land, Svalbard: Palaeogeography, Palaeoclimatology, Palaeoecology, v. 130, p. 163–175.
Ditchfield, P. W., Marshall, J. D., and Pirrie, D., 1994, High latitude palaeotemperature variation: new data from the Tithonian to Eocene of James Ross Island, Antarctica: Palaeogeography, Palaeoclimatology, Palaeoecology, v. 107, p. 79–101.
Dolginow, J., and Kropatschjow, S., 1994, Abriß der Geologie Rußlands und angrenzender Staaten: Stuttgart, Schweitzerbart, 174 p.
Emiliani, C., and Shackleton, N. J., 1974, The Brunhes epoch: isotopic paleotemperatures and geochronology: Science, v. 183, p. 511–514.
Fleming, C. A., and Kear, D., 1960, The Jurassic sequence at Kawhia Harbour, New Zealand (Kawhia Sheet, N73): New Zealand Geological Survey Paleontological Bulletin, v. 67, p. 1–20.
Fritz, P., 1967, Oxygen and carbon isotopic composition of carbonates from the Jura of South Germany: Canadian Journal of Earth Sciences, v. 4, p. 1247–1267.
Gradstein, F. M., Agterberg, F. P., Ogg, J. G., Hardenbol, J., vanVeen, P., Thierry, J., and Huang, Z., 1994, A Mesozoic time scale: Journal of Geophysical Research, v. 99 B12, p. 24151–24074.
Geosecs, 1987, GEOSECS Atlantic, Pacific, and Indian Ocean expeditions. Volume 7: Shore based data and graphics: Washington, D.C., National Science Foundation, 200 p.
Hagelberg, T. K., Bond, G., and deMenocha1, P., 1994, Milankovitch band forcing of sub-Milankovitch climate variability during the Pleistocene: Paleoceanography, v. 9, p. 545–558.
Hallam, A., 1985, A review of Mesozoic climates: Journal of the Geological Society of London, v. 142, p. 443–445.
Harland, W. B., Armstrong, R. L., Cox, A. V., Craig, L. E., Smith, A. G., and Smith, D. G., 1990, A geologic time scale: Cambridge, Cambridge University Press, 263 p.
Helby, R., Wilson, G. J., and Grant-Mackie, J. A., 1988, A preliminary biostratigraphy study of Middle to Late Jurassic dinoflagellate assemblages from Kawhia, New Zealand: Memoir of the Association of Australasian Palaeontologists, v. 5, p. 125–166.
Holser, W. T., Magaritz, M., and Ripperdan, R. L., 1996, Global isotopic events, *in* Walliser, O. H., editor, Global events and event stratigraphy in the Phanerozoic: Berlin, Springer, p. 63–88.
Huber, B. T., Hodell, D. A., and Hamilton, C. P., 1995, Middle-Late Cretaceous climate of the southern high latitudes: stable isotopic evidence for minimal equator-to-pole thermal gradients: Geological Society of America Bulletin, v. 107, p. 1164–1191.
Hudson, J. D., and Anderson, T. F., 1989, Ocean paleotemperature and isotopic compositions through time: Transactions of the Royal Society of Edinburgh, Earth Sciences, v. 80, p. 183–192.
Jenkyns, H. C., Gale, A. S., and Corfield, R. M., 1994, Carbon and oxygen-isotope stratigraphy of the English chalk and Italian Scaglia and its paleoclimatic significance: Geological Magazine, v. 131, p. 1–34.
Jones, C. E., Jenkyns, H. C., Coe, A. L., and Hesselbo, S. P., 1994, Strontium isotopic variations in Jurassic and Cretaceous seawater: Geochimica et Cosmochimica Acta, v. 58, p. 3061–3074.
Jones, C. E., Jenkyns, H. C., and Hesselbo, S. P., 1994, The strontium isotopic composition of Early Jurassic seawater: Geochimica et Cosmochimica Acta, v. 58, p. 1285–1301.
Land, L. S., 1995, Oxygen and carbon isotopic composition of Ordovician brachiopods: implications for coeval sea water: Discussion: Geochimica et Cosmochimica Acta, v. 59, p. 2843–2844.
Lini, A., Weissert, H., and Erba, E., 1992, The Valanginian carbon isotope event: a first episode of green house climate during the Cretaceous: Terra Nova, v. 4, p. 374–384.
Longinelli, A., 1969, Oxygen-18 variations in belemnite guards: Earth and Planetary Science Letters, v. 7, p. 209–212.
Lowenstam, H. A., 1961, Mineralogy, O-18/O-16 ratios, and strontium and magnesium contents of recent and fossil brachiopods and their bearing on the history of the oceans: Journal of Geology, v. 69, p. 241–260.
Machel, H. G., 1985, Cathodoluminescence in calcite and dolomite and its chemical interpretation: Geoscience Canada, v. 12, p. 139–147.
McConnaughey, T., 1989, ^{13}C and ^{18}O isotopic disequilibrium in biological carbonates. II. In vitro simulations of kinetic isotope effects: Geochimica et Cosmochimica Acta, v. 53, p. 151–162.

Milliman, J. D., 1974, Recent Sedimentary Carbonates; Part I: Marine Carbonates: Berlin, Springer, 375 p.
Morrison, J. O., and Brand, U., 1986, Geochemistry of recent marine invertebrates: Geoscience Canada, v. 13, p. 237–254.
Müller-Stoll, H., 1936, Beiträge zur Anatomie der Belemnoidea: Nova Acta Leopoldina Neue Serie, v. 4, p. 159–226.
Mutterlose, J., 1992, Migration and evolution of patterns of floras and faunas in marine early Cretaceous sediments of NW Europe: Palaeogeography, Palaeoclimatology, Palaeoecology, v. 94, p. 261–282.
Neuser, R. D., 1988, Zementstratigraphie und Kathodolumineszenz des Korallenoolith (Malm) im Südniedersächsischen Bergland: Bochumer geologische und geotechnische Arbeiten, v. 32, 172 p.
Norusis, M. J., 1985, SPSS-X advanced statistics guide: New York, McGraw-Hill, 505 p.
Pirrie, D., and Marshall, J. D., 1990, High-palaeolatitude Late Cretaceous palaeo-temperatures: new data from James Ross Island, Antarctica: Geology, v. 18, p. 31–34.
Podlaha, O. G., ms, 1995, Modellrechnungen auf der Basis hochauflösender Isotopenstratigraphie ($\delta^{13}C$, $\delta^{18}O$, $^{87}Sr/^{86}Sr$) des Jura und der Unteren Kreide (Bajoc-Barrême/Apt): Ph.D. thesis, Bochum, Ruhr-University, 256 p.
Popp, B. N., Anderson, T. F., and Sandberg, P. A., 1986, Brachiopods as indicators of original isotopic composition in some Paleozoic limestones: Geological Society of America Bulletin, v. 97, p. 1262–1269.
Reeder, R. J., and Grams, J. C., 1987, Sector zoning in calcite cement crystals: implications for trace element distribution in carbonates: Geochimica et Cosmochimica Acta, v. 51, p. 187–194.
Richter, D. K., and Zinkernagel, U., 1980, Zur Anwendung der Kathodolumineszenz in der Karbonatpetrographie: Geologische Rundschau, v. 70, p. 1276–1302.
Ruddiman, W. F., Raymo, M. E., Martinson, D. G., Clement, B. M., and Backman, J., 1989, Pleistocene evolution: Northern hemisphere ice sheets and North-Atlantic ocean: Palaeoceanography, v. 4, p. 353–412.
Sælen, G., 1989, Diagenesis and construction of the belemnite rostrum: Palaeontology, v. 32, p. 765–798.
Sælen, G., Doyle, P., and Talbot, M. R., 1996, Stable-isotope analyses of belemnite rostra from the Whitby Mudstone Fm., England: surface water conditions during deposition of a marine black shale: Palaios, v. 17, p. 97–117.
Sælen, G., and Karstang, T. V., 1989, Chemical signatures of belemnites: Neues Jahrbuch für Geologie und Paläontologie, Abhandlungen, v. 177, p. 333–346.
Savard, M., Veizer, J., and Hinton, R. W., 1995, Cathodoluminescence at low Fe and Mn concentrations: a SIMS study of zones in natural calcites: Journal of Sedimentary Research, v. 65A, p. 208–213.
Schlanger, S. O., and Jenkyns, H. C., 1976, Cretaceous oceanic anoxic events: causes and consequences: Geologie en Mijnbouw, v. 55, p. 179–184.
Shackleton, N. J., and Kennett, J. P., 1975, Paleotemperature history of the Cenozoic and the indication of the Antarctic glaciation: oxygen and carbon isotope analyses in DSDP sites 277, 279, 281: Initial Reports Deep Sea Drilling Project, v. 29, p. 742–755.
Smith, A. G., Hurley, A. M., and Briden, J. C., 1981, Phanerozoic paleocontinental world maps: Cambridge, Cambridge University Press, 102 p.
Spaeth, C., 1975, Zur Frage der Schwimmverhältnisse bei Belemniten in Abhängigkeit vom Primärgefüge der Hartelle: Paläontologische Zeitschrift, v. 49, p. 321–331.
Spaeth, C., Hoefs, J., and Vetter, U., 1971, Some aspects of isotopic composition of belemnites and related paleotemperatures: Geological Society of America Bulletin, v. 82, p. 3139–3150.
Swart, P. K., 1983, Carbon and oxygen isotope fractionation in Scleractinian corals: a review: Earth Sciences Review, v. 19, p. 51–80.
Thurow, J., and Kuhnt, W., 1986, Mid-Cretaceous of the Gibraltar Arch area. *in* Summerhayes, C. P., and Shackleton, N. J., editors, North Atlantic Palae-Oceanography: Geological Society of London Special Publication, v. 21, p. 423–446.
Urey, H. C., Lowenstam, H. A., Epstein, S., and McKinney, C. R., 1951, Measurement of paleotemperatures and temperatures of the Upper Cretaceous of England, Denmark and the Southeastern United States: Geological Society of America Bulletin, v. 62, p. 399–416.
Veizer, J., 1974, Chemical diagenesis of belemnite shells and possible consequences for paleotemperature determinations: Neues Jahrbuch für Geologie und Paläontologie, Abhandlungen, v. 147, p. 91–111.
—— 1983, Chemical diagenesis of carbonates: theory and application of trace element technique, in Arthur, M. A., Anderson, T. F., Kaplan, I. R., Veizer, J., and Land, L. S., editors, Stable isotopes in sedimentary geochemistry: Society of Economic Paleontologists and Mineralogists Short Course, v. 10, p. 3/1–3/100.
—— 1995, Oxygen and carbon isotopic composition of Ordovician brachiopods: Implications for coeval sea water: Reply: Geochimica et Cosmochimica Acta, v. 59, p. 2845–2846.
Veizer, J., Bruckschen, P., Pawellek, F., Diener, A., Podlaha, O. G., Carden, G. A. F., Jasper, T., Korte, C., Strauss, H., Azmy, K., and Ala, D., 1997, Oxygen isotope evolution of Phanerozoic sea water: Palaeogeography, Palaeoclimatology, Palaeoecology, v. 132, p. 159–172.
Veizer, J., and Fritz, P., 1976, Possible control of post-depositional alteration in oxygen paleotemperature determinations: Earth and Planetary Science Letters, v. 23, p. 255–260.
Veizer, J., Fritz, P., and Jones, B., 1986, Geochemistry of brachiopods: oxygen and carbon isotopic records of Paleozoic oceans: Geochimica et Cosmochimica Acta, v. 50, p. 1679–1696.
Veizer, J., and Hoefs, J., 1976, The nature of O^{18}/O^{16} and C^{13}/C^{12} secular trends in sedimentary rocks: Geochimica et Cosmochimica Acta, v. 40, p. 1387–1395.
Weber, J. N., 1967, Possible changes in the isotopic composition of the ocean and atmospheric carbon reservoir over geologic time: Geochimica et Cosmochimica Acta, v. 31, p. 2343–2351.
Weber, J. N., and Woodhead, P. M. J., 1970, Carbon and oxygen isotope fractionation in the skeletal carbonate of reef-building corals: Chemical Geology, v. 6, p. 93–117.

Wefer, G., 1985, Die Verteilung stabiler Isotope in Kalkschalen mariner Organismen: Geologisches Jahrbuch A, v. 82, p. 1–114.
Weissert, H., and Mohr, H., 1996, Late Jurassic climate and its impact on carbon cycling. Palaeogeography, Palaeoclimatology, Palaeoecology, v. 122, p. 27–43.
Wiedmann, J., Butt, A., and Einsele, G., 1978, Vergleich von marokkanischen Kreide-Küstenaufschlüssen und Tiefseebohrungen (DSDP): Stratigraphie, Paläo-environment und Subsidenz an einem passiven Kontinentalrand: Geologische Rundschau, v. 67, p. 454–508.
Williams, D. F., Lerchie, I., and Full, W. E., 1988, Isotope Chronostratigraphy: Theory and Methods: New York, Academic Press, 345 p.
Woodruff, R., Savin, S. M., and Douglas, R. E., 1981, Miocene stable isotope record: A detailed deep Pacific Ocean study and its paleoclimatic implications: Science, v. 212, p. 665–668.